Radiocarbon (2024), **66**, pp. 341–370
doi:10.1017/RDC.2024.44

CAMBRIDGE UNIVERSITY PRESS

RESEARCH ARTICLE

Problems of Dating Spread on Radiocarbon Calibration Curve Plateaus: The 1620–1540 BC Example and the Dating of the Therasia Olive Shrub Samples and Thera Volcanic Eruption

Sturt W Manning

Cornell Tree Ring Laboratory, Department of Classics, and Cornell Institute for Archaeology and Material Studies, Cornell University, Ithaca NY 14853, USA and The Science and Technology in Archaeology and Culture Research Center, The Cyprus Institute, 20 Konstantinou Kavafi Street, 2121 Aglantzia, Nicosia, Cyprus
Corresponding author: Sturt W Manning; Email: sm456@cornell.edu

Received: 02 August 2023; **Revised:** 03 January 2024; **Accepted:** 10 February 2024

Keywords: Bayesian modeling; calibration curve plateaus; radiocarbon dating; Thera eruption; Therasia olive shrub

Abstract

Determining calendar ages for radiocarbon dates, or ordered sequences of radiocarbon dates, that intersect with a plateau on the radiocarbon calibration curve can be problematic since, without additional prior constraints, the calendar age ranges determined will tend to spread across the plateau, yielding wide and less than useful calendar age probability densities and age ranges. Where possible, modeling analysis should seek to identify informative priors that act to restrict the otherwise poorly controlled spread of probability across plateaus. Such additional information may be available, among other sources, from the stratigraphy, the context, or the samples themselves. The recent dating of ordered sequences of radiocarbon dates on sections of branches of the same olive (*Olea europaea*) shrub from Therasia (southern Aegean) associated with the Minoan eruption of the Thera (Santorini) volcano (Pearson et al. 2023), which intersect with the plateau in the radiocarbon calibration curve ca. 1620–1540 BC, offers an example of the problem. A re-analysis adding some plausible informative priors offers a substantially better defined likely dating range and different conclusions. Instead of finding an inconclusive probability range "encompassing the late 17th and entire 16th century BC" followed by arguments for "indications of increased probabilities for a mid-16th century BC date for the eruption," a re-analysis incorporating appropriate informative priors identifies the likely date range as falling between the late 17th to early 16th centuries BC.

Introduction

Dating and Radiocarbon Calibration Curve Plateaus

Plateaus in the radiocarbon calibration curve inherently spread dating probability across wider calendar date ranges. Ironically, the application of Bayesian sequence analysis where a sequence has limited constituent ordered (relative) elements can exacerbate the problem. The prior information is an order of stratum/context B older than stratum/context A (so B > A), etc., but, on a plateau, this merely encourages the spread of the sequence across the plateau (unless there are sufficient members of the sequence to establish a specific placement). Worse, if the total length of the dated context (or set of contexts) is shorter than the temporal extent of the plateau, then analysis may fail to resolve the inherent ambiguities and thus not offer much greater calendar resolution than the non-modeled dates. In the absence of cases where longer sequences defined in calendar terms can be incorporated—like a tree-ring wiggle-match where plateau ambiguity can be resolved (e.g. Quarta et al. 2010; Meadows et al. 2014;

Manning et al. 2018c)—the only approaches to achieve dating that avoid "plateau spread" (where the ambiguities become cumulative, rather than being eliminated/resolved) is to add one or two forms of additional informative (constraining) prior information: (i) an association with the period before/after the plateau where dating is thus better constrained through stratigraphic, known-sequence (e.g. tree-ring series) or typological information, and/or (ii) prior knowledge of total sequence length and/or of any intra-sequence associations (e.g. Waddington et al. 2019; Meadows et al. 2020; Manning et al. 2020a; Manning and Birch 2022; Rose et al. 2022). In the absence of such forms of additional constraints, sequences of dates on a plateau will end up defining too wide a calendar age range and will likely end up suggesting dating probability that is either too old or too recent. In addition, given the inherent tendency to spread dating probability, Bayesian analysis of a sequence of dates across a plateau forms a prime case where boundaries must be employed to avoid a potentially wider spread of probability than is realistic, as highlighted by Steier and Rom (2000).

In general, in cases where there is a known sequence of several consecutive contexts (e.g.: . . . C > B > A), like stratigraphic contexts whether anthropogenic (archaeological) or natural, where the sequence length is greater than the length of the plateau or begins/ends before/after the plateau, then, although modeling may experience some probability spread across the plateau portion, these offer situations where properly constructed Bayesian Chronological Modeling (e.g. Bronk Ramsey 2009a; Bayliss 2009) integrating the prior knowledge (the known sequence) with the radiocarbon dating probability can serve to varying degrees to overcome what would otherwise have been calendar dating ambiguity. Work aimed at calendar resolution across the so-called Hallstatt Plateau 800–400 BC offers a good example (Hamilton et al. 2015); and, where forms of additional information can be added, the modeling may further improve resolution (e.g. Rose et al. 2022). In cases of defined sequence tree-ring series or multi-component ordered series from other natural archives like peat/salt-marsh sequences, both Bayesian and other frequentist approaches can enable good calendar determination to be achieved, especially as calibration curve resolution is improved (e.g., with reference to the Hallstatt Plateau, work like Fahrni et al. 2020), despite plateaus in the radiocarbon calibration curve (e.g. Bronk Ramsey et al. 2001; van de Plassche et al. 2001; Jacobsson et al. 2018)

More challenging are the cases without such a straightforward known sequence of distinct information from several consecutive contexts, in particular, where there is effectively just a single site context. Previous work has discussed and illustrated some potential methods to try to address and better resolve dating on a plateau in the radiocarbon calibration curve in such cases:

(a) Where suitable sample material is available, even a short (only several decades long) tree-ring-sequenced wiggle-match can be key if this can tie a particular sample to an area of the calibration curve and the last dated tree-ring of this sample can be related securely as defining a *terminus post quem* (TPQ) for the target date/context, or as defining the target date/context, or as defining a *terminus ante quem* (TAQ) for the target date/context. An example is the tree-ring wiggle match of the (extant) 57 tree-ring (calendar years) sample that allowed resolution of the dating of the Warminster site in Ontario, Canada, on the AD 1480–1630 plateau in the radiocarbon calibration curve (Manning et al. 2018a, 2019).

(b) Even where no samples suitable for a tree-ring-sequenced wiggle-match are available, the presence of a random selection of wood-charcoal samples in a context assemblage, with this population offering TPQ data encompassing a range (older to nearer contemporary) of "post" values in the TPQ, can serve to resolve ambiguity, either by linking part of the TPQ to the period before the plateau and hence placing the target context to be dated in the earlier part of the plateau, or, because the charcoal samples act to place the TPQ also on the plateau and thus the TPQ informs the dating of the target context as later on the plateau. An example here is the placement and dating of the Jean-Baptiste Lainé (Mantle) site in Ontario, Canada (Manning and Birch 2022) towards the end of the AD 1480–1630 plateau.

(c) Examination and consideration of the details of the target context and assemblage may further inform on dating parameters, in particular on the likely period(s) of time involved within the

https://doi.org/10.1017/RDC.2024.44 Published online by Cambridge University Press

context, or overall as regards the total length of a context (e.g. Meadows et al. 2020; Manning et al. 2020a; Rose et al. 2022). One example applied to dating 16th–17th century AD Iroquoian villages is ethnohistoric and archaeological evidence informing that typical overall village occupation periods were relatively short, and thus a plausible total duration can be set as the assumption for such dated contexts (the overall village occupation) and used to constrain a dating model (see Manning et al. 2020a; Birch et al. 2021). Another such approach employed archaeogenetic prior information (kinship relations among the burial population and likely additional periods of time from sample date to age at death estimates) to better resolve the chronology of a Late Neolithic (later 4th millennium BC) funerary context at Niedertiefenbach, Germany (Meadows et al. 2020).

Context and Woody Plant Growth Properties (Even When Not a "Wiggle-Match") as Prior Information

As noted above, where a defined tree-ring sequence is available for a wiggle-match, this can often offer increased dating resolution for a radiocarbon calibration curve plateau situation. But there are various woody plants that do not produce visible or easily identifiable annual growth rings suitable for a defined sequence analysis: the olive (*Olea europaea*) is a well-known example relevant to many Mediterranean contexts (Cherubini et al. 2013). However, developing the logic and examples described above, and especially in case (c), even the approximate ordered sequence information available from the properties of woody plant growth (from inner/older to outer/more recent samples) integrated with the sample's/site's context may still be able to provide prior information which can help resolve calendar dating, and in particular avoid excessive "plateau spread" for a context lying across a plateau in the radiocarbon calibration curve.

The recent publication of radiocarbon dates offering sequences (inner to outer growth segments) from four samples of olive wood from different pieces of the same olive shrub from Therasia in the southern Aegean (Pearson et al. 2023; for the archaeological context of the olive shrub, see also Sbonias et al. 2020) offers a good case study that highlights and encompasses all aspects of the problems associated with plateau spread for radiocarbon dating—and thus also an opportunity to consider approaches to address this issue. In the Pearson et al. (2023) paper the four olive branch samples, 88-3, 88-2, 88-1 and 72-2, are each considered as separate sequences, from inner growth to outer growth (or bark) segments in OxCal, and conclusions are drawn from the modeled age ranges of the last (outer) growth segments—argued to be associated with (killed by), and so relevant to, the dating of the Minoan eruption of the Thera or Santorini volcano. The modeled calendar probability spreads widely across the period from the later 17th century to later 16th century BC due to the plateau in the radiocarbon calibration curve (see Figure 1).

This case illustrates the relevance of several of the points noted above. First, the example OxCal code (Pearson et al. 2023: Supplementary Information, M3) indicates no use of Boundaries around the sequences. While a relatively minor to negligible issue here, in each case this leads consistently to slightly differing and overall slightly less well-defined dating probabilities for the ordered sequences (especially if we compare results from Difference queries describing the calendar years period between first and last dates for each sample comparing the no-Boundaries versus with-Boundaries models for each olive wood sample): Figure 1, Table 1. Second, the modeled ordered sequences reported indicate periods of calendar time, from the inner segment to outer segment/bark, that are typically rather longer than would reasonably be anticipated from the descriptions of the samples and the indications of growth features mentioned and this issue is especially noticeable in some cases where no boundaries are employed (as in Pearson et al. 2023). A particular instance is sample 88-3, stated to be an 8 mm round wood shoot with ca. 3–10 growth bands (Pearson et al. 2023: Fig. 2a, Table 2). This is clearly a sample of no more than a few years of total growth (whether the stated growth bands represent annual or

https://doi.org/10.1017/RDC.2024.44 Published online by Cambridge University Press

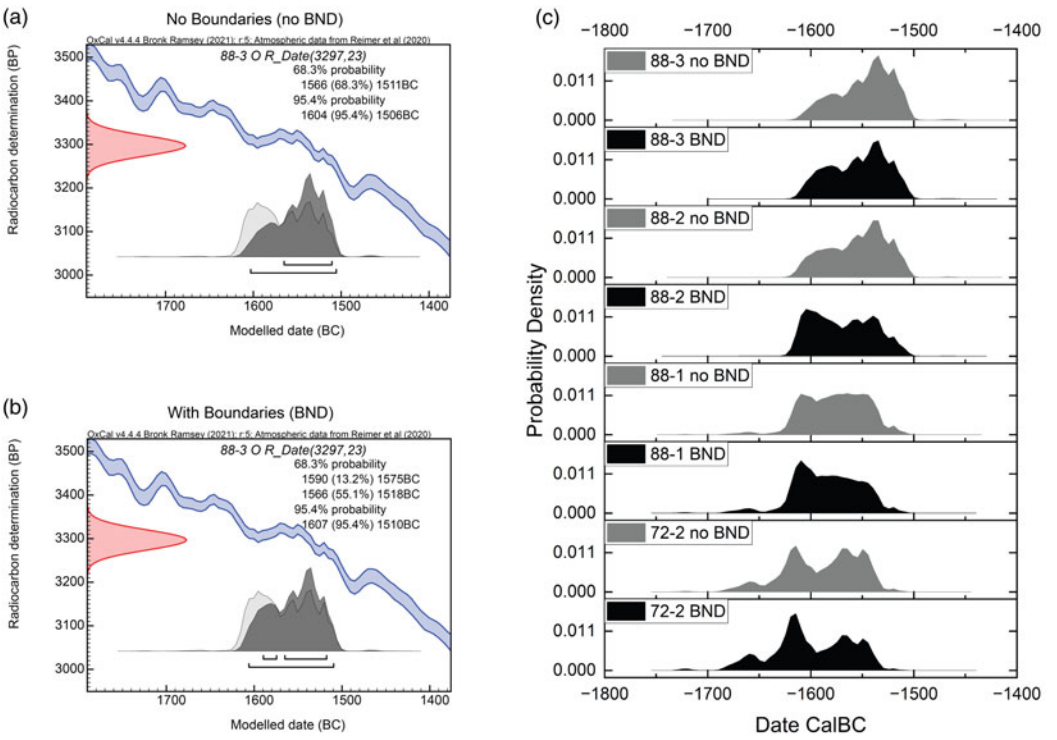

Figure 1. *Comparisons of the modeled probability densities for the Therasia outer/bark dates from the ordered Sequences from each olive wood sample using IntCal20 without use of Boundaries (as in Pearson et al. 2023) and with Boundaries.* ***a.*** *The modeled outer edge sample/date from 88-3, the olive shoot with no use of Boundaries with the Sequence analysis versus IntCal20 and the 16th century BC plateau.* ***b.*** *As a but using Boundaries.* ***c.*** *Each modeled Therasia outer/bark date from the four ordered Sequence models for each olive wood sample, first without and then second with use of Boundaries. Data from OxCal 4.4.4 and IntCal20 with curve resolution set at 5 years.*

intra-annual growth increments: see Methods below). But the "no boundaries model" reports a calendar years difference comparing the dating probabilities for the inner and outer segments with a median value of 35 years, contrasted with the model using boundaries which reports a difference with a median of 20 years: Table 1. This observation implies that some overall time constraint is appropriate/necessary. In turn, in cases where inner segments offer ages indicative of a pre-plateau 17th century BC date placement, application of a suitable constraint might serve to reduce the subsequent "plateau spread". Third, all the sample sequences end close to or at outermost growth increments or bark (intact juvenile bark in the case of sample 88-3) and the samples are all argued to have been killed by the Thera volcanic eruption (Pearson et al. 2023), similar to the previous case of an olive tree branch found on Thera itself (Friedrich et al. 2006, 2014). There is thus an important association available as prior information, likely placing all these outermost growth segments and/or bark (of the same olive shrub) close in calendar time and so offering an additional constraint from several data, and potentially offering control against any outlying value(s)—whereas treating each small sequence of radiocarbon dates entirely separately loses this temporal coalescence and maximizes "plateau spread" or any outlier effect.

This paper therefore re-examines the Therasia olive wood case and considers possible approaches to better date these samples addressing the problems noted above through the introduction of some informative priors into the analysis. The topic applies generally to dating across plateaus on the radiocarbon calibration curve, and specifically to current debate trying to narrow the dating range of the massive mid-second millennium BC eruption of the Thera (Santorini) volcano in the southern Aegean

https://doi.org/10.1017/RDC.2024.44 Published online by Cambridge University Press

Table 1. *The calendar date ranges for the outer segment or bark from the ordered sequence examples from Pearson et al. (2023: Fig. 5) for the Therasia olive samples run (as in Pearson et al. 2023) with IntCal20 and curve resolution set at 5 years (as in Pearson et al. 2023), comparing the results from Sequences run without Boundaries (as in Pearson et al. 2023) versus the same sequences but run with uniform probability Boundaries (see also Figure 1) and the results of a Difference query for the period of time in calendar years between the outer (most recent) dated segment and the inner (oldest) dated segment in each case. OxCal code and data in the Supplementary Material.*

Test, Estimated growth bands	Model	Pearson et al. 2023 (no "offset") 68.3% hpd; **95.4% hpd** date range BC	Difference Query (outer element minus inner element), Median, 68.3% hpd, **95.4% hpd**	Sequence with Boundaries 68.3% hpd; **95.4% hpd** date range BC	Difference Query (outer element minus inner element), Median, 68.3% hpd, **95.4% hpd**
722_OS_NB, ca. 54 inconsistent growth bands	Ordered Sequence	1627–1602 (24.4%), 1586–1542 (43.9%); **1670–1533**	*62 years* *3 to 90 years* ***–2 to 151 years***	1632–1600 (35.0%), 1584–1544 (33.3%); **1674–1536**	*36 years* *–2 to 61 years* ***–2 to 126 years***
881_OS-NB, ca. 40 indistinct growth bands	Ordered Sequence	1615–1599 (16.1%) 1591–1542 (52.2%); **1627–1519**	*107 years* *55 to 155 years* ***17 to 196 years***	1620–1557; **1665–1660 (0.6) 1635–1518 (94.8)**	*88 years* *32 to 133 years* ***3 to 180 years***
882_OS_WB, ca. 76-81 inconsistent growth bands	Ordered Sequence	1586–1575 (8.8%), 1569–1517 (59.5%); **1610–1510**	*105 years* *60 to 147 years* ***23 to 196 years***	1614–1577 (39.5%), 1565–1535 (28.7%); **1619–1517**	*65 years* *7 to 96 years* ***–2 to 150 years***
883__OS_NB, ca. 3-10 growth bands	Ordered Sequence	1566–1511; **1604–1506**	*35 years* *1 to 57 years* ***–2 to 96 years***	1590–1575 (13.1%), 1566–1518 (55.2%); **1607–1510**	*20 years* *–2 to 36 years* ***–2 to 81 years***

(Supplementary Material, Figure S1). This eruption is regarded as a key cultural marker horizon for the Aegean and East Mediterranean region, and its direct and indirect impacts on the Aegean region and the Minoan civilization of the nearby island of Crete have been much discussed (Driessen and Macdonald 1997; Manning 1999; Warburton 2009; Bietak and Höflmayer 2007; Doumas et al. 2015; Höflmayer 2012; Manning et al. 2014; Pearson et al. 2018, 2023; Driessen, 2019; Şahoğlu et al. 2021; Manning 2022). Years of debate have contested the date of the eruption. The discussion thus ends with brief consideration of the relevance of the Therasia samples and their analysis to the debate over the dating of the Thera (or Santorini) eruption when appropriate priors are included in the analysis. It is argued that the dating picture then becomes clearer. Recent radiocarbon-based arguments for a mid-16th century BC range turn out to be largely a product of the plateau in the radiocarbon calibration curve at this time when data are used without appropriate dating constraints. This in turn highlights the relevance of developing and applying methods that allow better calendar resolution in periods with plateaus in the radiocarbon calibration curve.

Methods

No new data are reported in this paper. Radiocarbon data employed come from published sources, principally the Therasia data in Pearson et al. (2023). The main sites/locations mentioned in the paper are indicated in the map in Figure S1 in the Supplementary Material. Analysis employs the OxCal software (Bronk Ramsey 2009a; 2009b) version 4.4.4 and the IntCal20 radiocarbon calibration curve (Reimer et al. 2020)—which is now extremely well-defined by a very large dataset from several laboratory measurement programs for the relevant period 1700–1500 BC—with curve resolution set at and stated as either 1 year (r1) or 5 years (r5) (as in Pearson et al. 2023) or 20 years (r20) (see further below). OxCal models (runfiles) and the data employed are listed in the Supplementary Material. To ensure good convergence in each model run reported, the kIterations value was increased from the default x100 (to 3000) and to x1000 (to 30000) for the DR runs reported (see below). Where all data, and the model overall, showed good OxCal Agreement values, no Outlier model was employed. Typical model results are reported from several runs. The 68.3% and 95.4% highest posterior density, hpd, calendar ranges can vary by ca. 0 to 1 or 2 years across individual runs (similarly probabilities, where sub-ranges occur, can vary, usually within 0-1%). From this point on, OxCal command terms, like Sequence, Difference, Phase, etc., are capitalized.

In the past it has been suggested that perhaps the organic materials from Thera were contaminated by volcanic carbon dioxide (CO_2), and thus yield radiocarbon ages that are too old (e.g. Wiener 2012). However, comparison of radiocarbon dates—such as the dates on the Therasia olive shrub—with radiocarbon dates on contemporary samples from contexts associated with the Thera eruption or its impacts from elsewhere in the Aegean well away from Thera allow us to test for, and dismiss, this concern (Manning 2022; Pearson et al. 2023). In further general support the case of the earlier 1st millennium AD Taupo volcanic eruption in New Zealand may also be noted: here independent ice-core chronology has recently supported/confirmed the date derived from radiocarbon dating of associated regional tree-ring series and other samples and refuted a suggestion that there was perhaps a substantial volcanic CO_2 age bias across a large area (Piva et al. 2023).

Olive Growth Bands

The Therasia olive samples are reported as exhibiting growth bands: sample 88-3 has ca. 3–10 growth bands ending in juvenile bark, sample 88-2 has ca. 76-81 inconsistent growth bands ending in bark, sample 88-1 has ca. 40 indistinct bands, and sample 72-2 has ca. 54 inconsistent growth bands (Pearson et al. 2023: Table 2). The key issue is what the reported growth bands (often indistinct) represent in temporal terms. *Olea europaea* is a species with high plasticity in xylogenesis and is therefore capable of opportunistically growing new wood cells when growing conditions are favorable (as typical of

https://doi.org/10.1017/RDC.2024.44 Published online by Cambridge University Press

Table 2. *Modeled calendar age ranges for the three outermost and one bark segment of the four Therasia samples and then for the Boundary labelled "Eruption" that immediately follows a Phase comprising each of the modeled outer/bark dates from the different model versions and which should describe the date range for the Thera eruption (see Methods).*

Model	OxCal Am/Ao	hpd	88-3 last, Date BC	88-2 bark (likely same as Thera eruption date), Date BC	88-1 last, Date BC	72-2 last, Date BC	Boundary "Eruption", Date BC
A_20r1	128/127	68.3%	1613–1598	1614–1599	1617–1601	1619–1599	1611–1592
		95.4%	1619–1580	1621–1581	1625–1590	1635–1576	1616–1571
A_20r5	125/124	68.3%	1614–1597	1616–1596	1617–1601	1621–1598	1611–1591
		95.4%	1620–1579	1621–1581	1626–1589	1636–1575	1617–1571
A_20r20	101/101	68.3%	1617–1583	1621–1581	1621–1589	1623–1587	1613–1581
		95.4%	1631–1567	1631–1569	1639–1577	1641–1561	1621–1559
A_20r1U	127/126	68.3%	1614–1602	1615–1602	1615–1603	1616–1602	1611–1597
		95.4%	1618–1592	1619–1592	1621–1593	1622–1592	1615–1587
A_10r1	127/126	68.3%	1614–1601	1614–1601	1615–1602	1617–1601	1611–1598
		95.4%	1618–1589	1620–1589	1623–1591	1626–1587	1616–1584
A_20_TOr1	162/160	68.3%	1613–1601	1614–1602	1616–1603	1618–1601	1611–1597
		95.4%	1618–1588	1620–1589	1624–1593	1632–1587	1615–1582
A_20_TOr5	150/149	68.3%	1614–1600	1615–1600	1617–1602	1619–1601	1611–1596
		95.4%	1620–1589	1621–1587	1626–1591	1632–1587	1616–1581
A20_TOr5U	150/149	68.3%	1615–1602	1616–1602	1616–1603	1617–1604	1612–1598
		95.4%	1619–1596	1620–1595	1621–1596	1622–1606	1616–1590
A_20_TOr20	101/101	68.3%	1615–1587	1617–1587	1619–1591	1621–1589	1613–1587
		95.4%	1631–1575	1633–1577	1639–1581	1639–1573	1631–1563
A_20DRr1	125/124	68.3%	1612–1598	1613–1598	1613–1599	1614–1599	1609–1593
		95.4%	1617–1585	1618–1585	1620–1586	1621–1584	1615–1580
A_20DRr5	123/122	68.3%	1612–1598	1613–1598	1614–1598	1615–1597	1609–1592
		95.4%	1619–1586	1620–1586	1621–1586	1621–1584	1616–1579
A_20DRPr1	116/114	68.3%	1610–1593	1610–1594	1611–1594	1611–1593	1606–1588

(*Continued*)

Table 2. (*Continued*)

Model	OxCal Am/Ao	hpd	88-3 last, Date BC	88-2 bark (likely same as Thera eruption date), Date BC	88-1 last, Date BC	72-2 last, Date BC	Boundary "Eruption", Date BC
		95.4%	1615–1578 (90.6) 1560–1554 (1.7) 1546–1535 (3.2)	1616–1578 (90.5) 1561–1555 (1.5) 1547–1536 (3.4)	1618–1581 (90.2) 1561–1555 (1.4) 1549–1536 (3.9)	1618–1578 (90.4) 1560–1556 (1.0) 1550–1536 (4.0)	1612–1574 (90.6) 1556–1552 (0.9) 1545–1531 (3.9)
A_20TOr5_LnN	151/151	68.3%	1615–1602	1616–1602	1616–1602	1617–1603	1613–1601
		95.4%	1619–1595	1620–1595	1621–1596	1623–1595	1617–1592
A_20TOr1_LnN	169/167	68.3%	1614–1605	1615–1606	1615–1606	1616–1606	1612–1603
		95.4%	1618–1599	1618–1599	1620–1599	1622–1598	1616–1596
B_20r1	122/125	68.3%	1610–1592	1611–1592	1614–1596	1616–1589	1607–1585
		95.4%	1615–1575	1617–1575	1622–1584	1629–1571	1613–1566
B_20r5	121/123	68.3%	1611–1590	1611–1591	1615–1594	1616–1590	1607–1585
		95.4%	1617–1573	1619–1574	1623–1583	1630–1571	1614–1565
B_10r1	120/123	68.3%	1611–1594	1611–1595	1613–1597	1614–1595 (65.2%) 1593–1592 (3.1%)	1608–1590
		95.4%	1615–1581	1616–1581	1619–1584	1623–1579	1613–1576
C_20r1	124/127	68.3%	1612–1597	1613–1597	1616–1601	1618–1598	1609–1592
		95.4%	1617–1581	1619–1582	1625–1591	1633–1579	1614–1573
C_20r5	122/124	68.3%	1613–1597	1614–1596	1616–1601	1619–1597	1610–1590
		95.4%	1619–1580	1621–1580	1626–1590	1635–1577	1616–1570
C_10r1	123/125	68.3%	1612–1600	1613–1600	1615–1601	1615–1600	1610–1596
		95.4%	1617–1588	1619–1588	1622–1592	1625–1587	1615–1584

Mediterranean species where growth is modulated by local climate and environmental conditions, and particularly soil moisture availability: Deslauriers et al. 2017). Hence olives have been stated to be problematic for dendrochronology as no regular, annual, growth increment can be recognized in many cases, and instead intra-annual density fluctuations are observed or anticipated (Cherubini et al. 2003, 2013; Kuniholm 2014). However, in the Mediterranean, olives are observed generally to exhibit growth (cambial activity) from late spring (e.g. April) right through the autumn to the start of winter (December): typically, there is a major growth spurt in xylogenesis from late spring to earlier summer (starting about April), then a quieter period in peak summer, before a second period of increased activity in the autumn (e.g. September-October) (Liphschitz and Lev-Yadun 1986; Drossopoulos and Niavis 1988a; 1988b; Chiraz 2013; Luz et al. 2014; Ehrlich et al. 2021). This sometimes enables annual increments to be recognized, whether by visual analysis or via stable isotope or radiocarbon (Camarero et al. 2021; Ehrlich et al. 2021), but often this is not possible from visual inspection (Cherubini et al. 2013).

The sum of these observations is that it is likely that the growth bands recognized in the Therasia olive wood constitute a total maximum age for a (complete) stem: since some to many (50% or more) of the growth bands observed are in all probability in fact intra-annual density fluctuations (and not solely annual increments), and hence the real calendar ages are less than the total number of observed growth bands (perhaps likely somewhere between 50%–100%). When considering a Sequence analysis of inner growth increment versus outer growth increment, it is therefore plausible that (i) the maximum total calendar age span is less than or equal to the maximum observed number of growth bands, and (ii) the realistic calendar age span is almost certainly less than the total maximum growth band count (Model A), perhaps somewhere between a 75% value ± 25% (Model B) to a 50% value ± 25% (Model C). These three scenarios are used in the analyses reported below.

Modeling

Each Therasia olive sample offers a temporal Sequence from (a) inner growth segments to (b) outer growth segments dated and then in one case to (c) bark dated. This can be modeled as an ordered Sequence within Boundaries (with a uniform probability assumption applied, but see also below). Each Sequence then has a maximum plausible calendar length defined by the observed growth bands. The dates for sample 88-3 comprised the pith and the outer edge. Thus the ca. 3–10 growth bands count applies directly. I use the maximum value of 10 to be conservative, hence the maximum time span is 10 years, the 75% ± 25% = 8 ± 2 years, and 50% ± 25% = 6.5 ± 2 years. Sample 88-2 has ca. 76–81 growth bands and the samples dated comprised the inner ca. 5 growth bands and ca. 5 outer-most growth bands and the bark. Hence the maximum time span from the mid-point of the inner sample (notional growth band 3) to bark (notional maximum growth band 82) is approximately at most 79 years, the 75% ± 25% = 59 ± 20 years (rounding), and 50% ± 25% = 40 ± 20 years. Sample 88-1 has ca. 40 growth bands, the inner date was on pith plus growth bands 1–4 and the outer date on the 3 outer growth bands. Hence the maximum time span from the mid-point of the inner sample (notional growth band 2 to 3) to the mid-point of the outer sample (notional growth band 39) is approximately at most 37 years, the 75% ± 25% = 28 ± 9 years (rounded), and 50% ± 25% = 19 ± 9 years. Sample 72-2 has ca. 54 growth bands, the inner date was on 4 inner-most growth bands and the outer date on the 5 outer-most growth bands. Hence the maximum time span from the mid-point of the inner sample (notional growth band 2.5) to mid-point of the outer sample (notional growth band 52) is approximately at most 50 years (rounded up), the 75% ± 25% = 37 ± 12 years, and 50% ± 25% = 25 ± 12 years. Each of these possible total time periods can be modeled via a Difference query between modeled inner and outer/bark dates with the appropriate constraints applied of (with sample 88-3 as the example): U(0, 10), N(8, 2) and N(6.5, 2).

The dates of the outer growth increments or bark should all lie close to the time growth stopped (i.e. the time when the olive shrub was killed) and this is associated with (caused by) the Thera volcanic

https://doi.org/10.1017/RDC.2024.44 Published online by Cambridge University Press

eruption (Pearson et al. 2023). For sample 88-3 (the shoot with outer date on outermost edge where there was juvenile bark) the outer date should be directly the same as the date of the eruption. The bark date for sample 88-2 may also reflect this last year although it may incorporate carbon from previous years in addition (Pearson et al. 2023). The other two outer dates are respectively 1 growth increment and 2 growth increments away from what are described as a "clear outer edge" (88-1) and an "intact outer edge" (72-2). All should thus set very close *terminus post quem* (TPQ) estimates for the date for the eruption (probably within at most ca. 2 years) and also, as a set of such associations, offer an additional prior for our models. The set of outer/bark ages may therefore be modeled as a Phase in OxCal with an exponential distribution towards the end of the Phase with the Boundary immediately following this Phase representing an approximation for the date of the Thera volcanic eruption using a Tau_Boundary paired with a Boundary in OxCal. Further, the overall calendar time period involved across the Phase of outer dates must be short (likely a few growth increments and so at most a few years). We may therefore constrain the time constant for the exponential distribution (the parameter Tau), assigning a prior. Given this time period appears to represent only 0–2 growth bands, it likely represents no more than about 2 years; hence a very conservative choice would be ($\times$10) a uniform prior between 0 and 20 years, and this is used in Models denoted with the addition of _20. A more realistic value might be a uniform prior between 0 and 10 years. This is used where model names are denoted with the addition of _10. The constraint on the time constant is a key issue, illustrated in a test considering uniform prior values of 0–5, 0–10, 0–20, 0–30 and 0–50 years and no time constant at all (see Discussion). As a test for how important the exponential assumption is, model versions (of A_20r1 and A_20TOr5) without the Tau_Boundary assumption are also included (A_20r1U and A_20TOr5U) (Note: the addition in a model name of "TO" indicates that the radiocarbon data from the previously published Thera Olive sample, see Friedrich et al. 2006, are included in this dating model: see below and see Supplementary Material). Here instead a uniform prior of 0–20 years is applied to a Difference query between the start and end Boundaries of the Phase containing the modeled outermost/bark dating probabilities (see Supplementary Material). Finally, an alternative to the fixed limits of a uniform prior assumption is considered: using instead a log-normal (LnN) distribution to capture the assumption that we expect all the outermost growth increment/bark Therasia olive shrub samples to date within a very similar period of just a couple of years, but without a hard upper limit if in fact the data themselves indicate a longer duration than expected. The form `LnN(ln(3),ln(2))`; where the expected mode value is around 2 years, the median value is around 3 years, and the 95.4% hpd range extends from <1 year to towards 10 years appears suitable (models denoted as _LnN).

Therasia Olive ^{14}C Offset?

Pearson et al. (2023) argue for the relevance of a small (13.7 ± 2 ^{14}C years) offset between measurements on the Therasia olive samples and IntCal20. This is an indirect argument. Pearson et al. observe that there is a 13.7 ± 2 ^{14}C years offset between a time-series of measurements on juniper from the central Anatolian plateau run at Arizona versus IntCal20. They then suggest the assumption that the olive samples from Therasia share this offset "[d]ue to the common laboratory factors and latitude". The laboratory is common. What is not common is the growing circumstances and thus timing of the incorporation of radiocarbon into the respective wood. Anatolian junipers on the central Anatolian plateau, or higher again in mountains, primarily grow (photosynthesize) earlier in the year through to (ending) early summer, thus they primarily represent a spring signal (and the intra-annual "low" in atmospheric ^{14}C levels). This is distinct from the later spring through summer to start autumn signal incorporated into most of the wood in the trees used to build the IntCal curve which in contrast represents the intra-annual "high" in atmospheric ^{14}C levels (Manning et al. 2018b, 2020b, 2020c). Hence an offset of the juniper data is plausible and the reported value is within the range of the known intra-annual seasonal variation. In contrast, olive growth is late spring through summer and also through the autumn (see above). Thus the period of olive growth and incorporation of radiocarbon likely is

https://doi.org/10.1017/RDC.2024.44 Published online by Cambridge University Press

broadly very similar to that represented by the trees currently used for IntCal and hence no substantive growing season offset should be assumed.[1]

The other possible issue is whether the reported Arizona laboratory values are systemically offset. Here the comparisons listed in Pearson et al. (2020) for data measured at Arizona (AA) versus data measured at ETH (Zürich) suggest that AA data on bristlecone pine exhibited a similar 13.6 ± 1.6 ^{14}C years offset, whereas AA data versus ETH on the same Irish oak was offset 6.8 ± 2.9 ^{14}C years. Thus it might be argued that Arizona data tends to be a little old in ^{14}C terms (*if* we assume ETH is closer to the real best value). However, before we then suggest incorporation of any such correction, we should note that all of the considerable amount of Arizona data on oak and bristlecone pine, and for the very period, 1700–1480 BC, relevant to the Therasia samples, is incorporated into IntCal20 (Pearson et al. 2020; Reimer et al. 2020)! Thus IntCal20 is already substantially "Arizona-informed" in the period 1700–1480 BC that is relevant to the Therasia samples—hence most of any possible Arizona laboratory offset is already substantially factored into IntCal20. The conclusion is that any remaining Arizona offset for these Therasia samples should be very small to non-existent. Adding any additional offset correction therefore appears inappropriate and only creates a likely strong bias. Nonetheless, as an exploratory check, Models A_20r1 and r5 were re-run (as Models A_20DRr1 and r5) including a Delta_R offset of 6 ± 3 ^{14}C years which should reasonably cover any residual Arizona offset not already factored into IntCal20 in the period 1700–1480 BC (based on the oak comparison which should be more relevant to the olive wood samples), and Model A_20r1 was further re-run with the larger Pearson et al. (2023) 13.7 ± 2 ^{14}C years offset as A_20DRPr1 (note: these DR models are reported from typical runs with kIterations = 30000).

Previous Thera Olive Sample

In addition to the Therasia olive samples there is the previously published Thera olive (TO) sample with a Sequence of radiocarbon dates on growth increments across the total of 72 growth increments recognized using 3D X-Ray tomography (Friedrich et al. 2006, 2014). It appears obvious to consider whether the information from this olive sample is compatible with the Therasia samples and data (also Pearson et al. 2023). Since the outermost edge of the TO sample (which likely represents the tree being killed by the eruption: Heinemeier et al. 2009) is 6 observed growth increments after the mid-point of the last dated sample, it seems appropriate to use the Boundary after the Sequence of data (approximately allowing for whatever exact time period, some years to ca. 6 years, give or take, is represented by the ca. 6 growth increments recognized after the mid-point of this last sample) as the best estimate for the death of this sample, and so the Thera eruption (as Friedrich et al. 2014). A uniform probability constraint is placed on the time period between the end Boundary (ETO) and the start Boundary (STO) of between 0 and 72 years (based on the observed number of total growth increments). This TO Sequence is then included in a variant of Model A_20r1 (Figure 2) labelled as Model A_20_TOr1.

[1] Postcript: In work published after the present paper was submitted, Raj et al. 2023b suggest that measurements on an olive sample from Israel might suggest a ^{14}C offset. But there is no secure dendrochronological basis to the calendar placements of the ^{14}C data reported: the caption to Raj et al. (2023b: Fig. 2) states "olive data points have been adjusted to match other Δ^{14}C records". The assessment, based just on such data matching, that the olive grew in spring and early summer in 1964, but then only late summer to winter in 1965, and did not grow in spring or summer in 1966, 1967 and 1968, appear difficult to reconcile, first, generally, with known olive tree growth behaviour (see Methods), and, second, with the detailed stable carbon isotope record measured and previously reported from the very same olive wood sample (Ehrlich et al. 2021: Fig. 2B). This stable isotope record seems to exhibit a spring (start) to a summer or later peak to fall/winter (end) δ^{13}C signal for each year and thus demonstrates photosynthesis and growth each year and across the later spring through autumn and not only at the different partial periods reported in Raj et al. (2023b). For example, the 1964 δ^{13}C record seems to have a largely symmetical shape and mid-year peak as does 1965, directly contrary to the claimed very different claimed growth periods from the radiocarbon 'matching' stated in Raj et al. (2023a). Therefore, the only conclusion is that the calendar timescale placements/associations reported in Raj et al. (2023b: Fig. 2) for the wood portions used for the ^{14}C measurements are likely not secure.

https://doi.org/10.1017/RDC.2024.44 Published online by Cambridge University Press

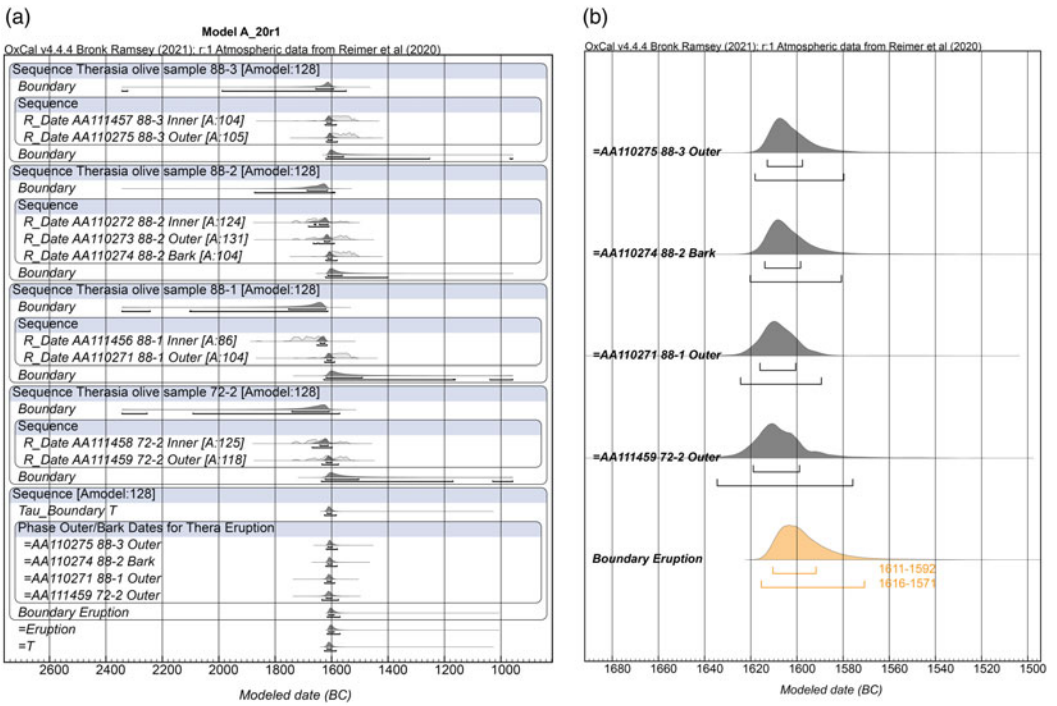

Figure 2. *Model A_20r1 (just the Therasia sample Sequences and Arizona AMS data).* ***a.*** *Model structure and results. Hollow, light-shaded, distributions show the non-modeled probability, the dark-shaded distributions show the modeled probability. The lines under the modeled distributions show the 68.3% and 95.4% high posterior density (hpd) ranges.* ***b.*** *Details of the modeled probabilities for the four outer or bark samples and for the Boundary "Eruption" that estimates the date the Therasia olive samples were collectively killed, and thus the date of the Thera volcanic eruption. Data from OxCal 4.4.4 and IntCal20 with curve resolution set at 1 year.*

Raj et al. (2023a) argue that, since the original Thera olive (TO) samples comprised blocks of wood containing a number of growth increments or likely years, then the radiocarbon dates obtained should be calibrated against a moving average calibration curve of similar chronological resolution (not that this is strictly known for such olive wood samples—see above). The difference is relatively small. Using the OxCal curve resolution function and settings at 1, 5, 10, 20 and 25 years the placement of the last dated segment of the Thera olive Sequence run in isolation (Hd-23588-24402 "rings" 60–72) changes respectively at 95.4% hpd from (whole range) 1625–1545 BC to 1626–1546 BC to 1629–1549 BC to 1639–1547 BC to 1644–1549 BC. However, the moving average curve shown in Raj et al. (2023a: Fig.1) includes a shift to more recent calendar years. The text notes that this is due to using the calendar age of the last ring in the block and not the mid-point (which appears inappropriate). A moving average should dampen wiggles and shape changes (e.g. lower ^{14}C ages on the earlier portions of slopes and raised ^{14}C ages on the later portions of slopes), but not create a parallel calendar-shifted curve (as shown e.g. for the period 1620–1600 BC in the moving average curve of Raj et al. 2023a: Fig.1). Results are reported here using curve resolutions of 1, 5 and 20 years, denoted as r1, r5, r20 for the versions of Model A, for comparisons, and are reported in Table 2.

The structure, results and calendar placements from Model A_20r1, and Model A_20TOr5, are shown as examples in Figures 2–4. OxCal runfiles for these two models and for examples of Models B and C applying the above sets of constraints are listed in the Supplementary Material. The modeled dates for the outer dated segment of each Therasia sample and the modeled dates for the Thera eruption

https://doi.org/10.1017/RDC.2024.44 Published online by Cambridge University Press

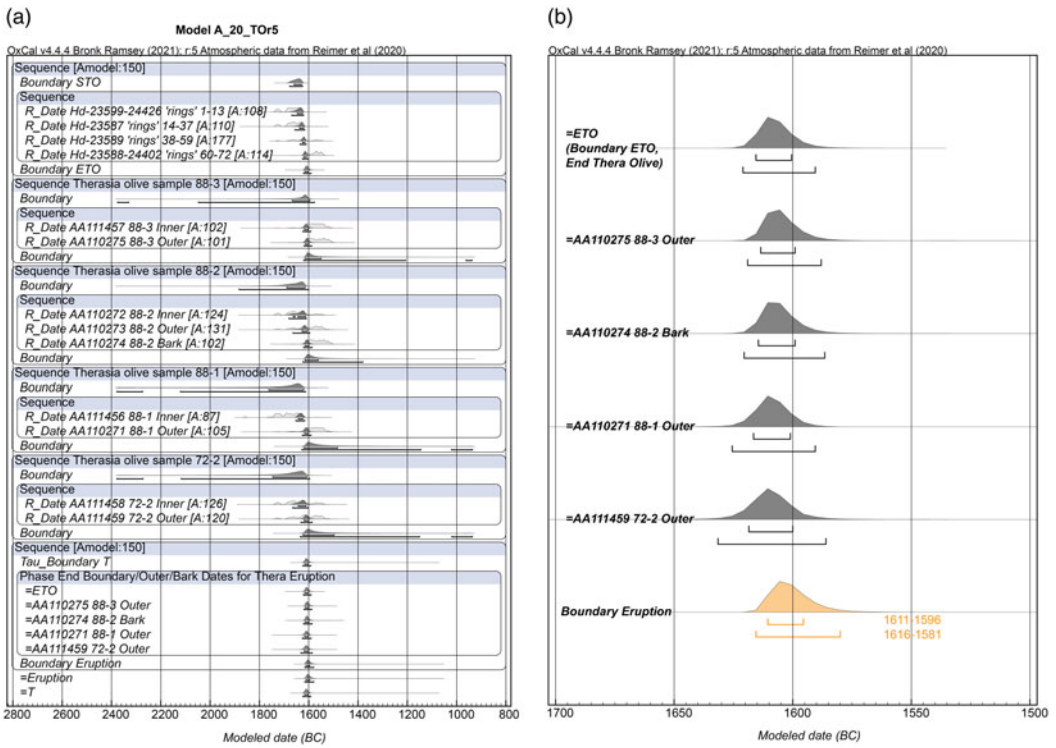

Figure 3. *Model A_20TOr5 (adding the Thera olive, TO, Sequence).* ***a.*** *Model structure and results. Hollow, light-shaded, distributions show the non-modeled probability, the dark-shaded distributions show the modeled probability. The lines under the modeled distributions show the 68.3% and 95.4% high posterior density (hpd) ranges.* ***b.*** *Details of the modeled probabilities for the five outer or bark samples and for the Boundary "Eruption" that estimates the date the Therasia olive samples and Thera olive sample were all collectively killed, and thus the date of the Thera volcanic eruption. Data from OxCal 4.4.4 and IntCal20 with curve resolution set at 5 years.*

derived from the Phase of these dates for each of the different model runs considered are listed in Table 2.

Results

The structure, results, and calendar placements from Model A_20r1 and Model A_20TOr5 are shown as examples in Figures 2–4. Figure S2 (Supplementary Material) illustrates that running the elements and model stages separately, versus together in one overall model as shown in Figure 3 (Model A_20_TOr5), and as the other models reported in Tables 2 and 3, achieves effectively identical results. The structure and results from Model B_20r5 and Model C_10r1 are shown as further examples in the Supplementary Material in Figures S3 and S4. The calendar dating probabilities for Model A_r1 run with a range of time constant values (and no time constant value) are shown in Figure 5. Finally, the Boundary representing the date of the Thera eruption using the alternative `LnN(ln(3),ln(2));` time constraint from Model A with calibration curve resolutions of 5 years and 1 year, and the fit of this assumption versus model results, are shown in Figure 6. The modeled calendar age ranges for the outermost segments/bark for the four Therasia samples, as well as the modeled Boundary that represents the end of a Phase comprising all four outer/bark dates (and in one case, Model A_20_TO, with the end Thera olive, TO, Boundary in addition) and so the date of the Thera eruption, are listed in Table 2. It is

https://doi.org/10.1017/RDC.2024.44 Published online by Cambridge University Press

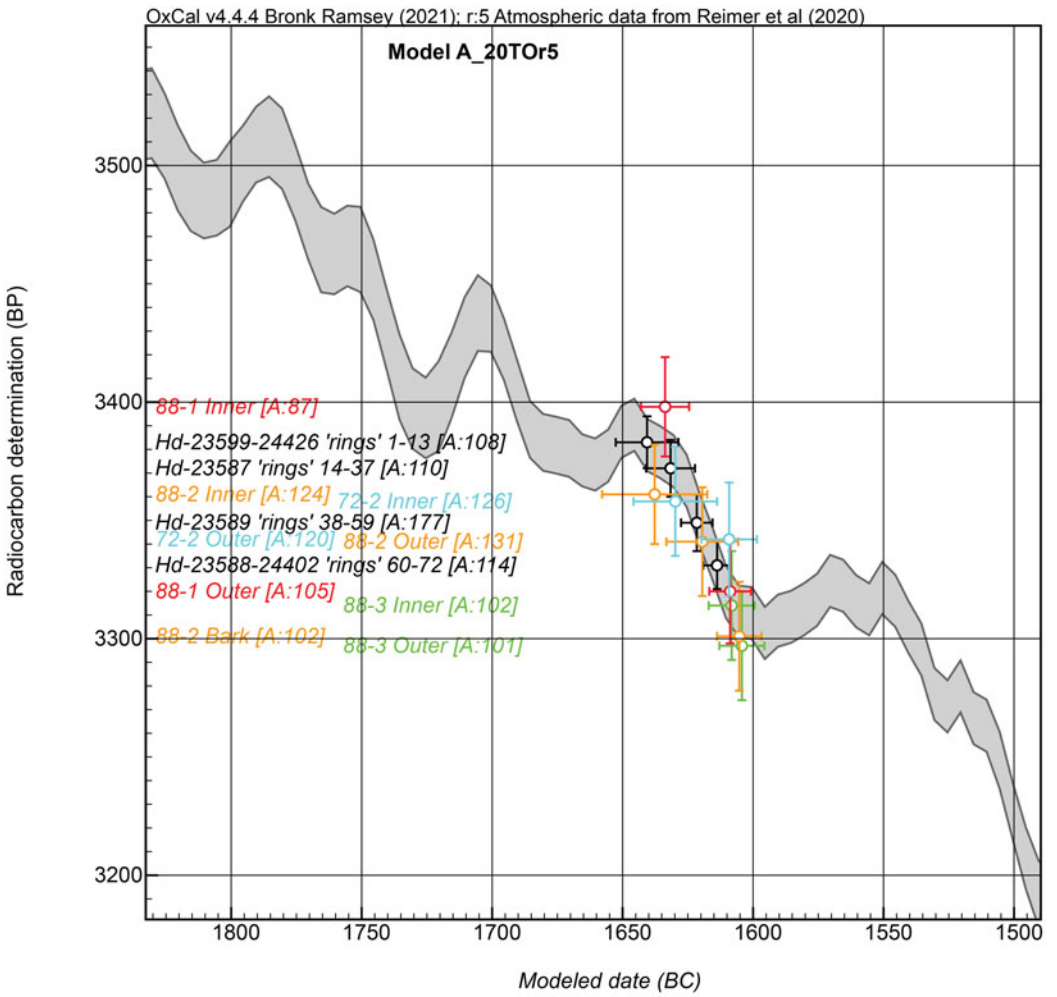

Figure 4. *Placement of the mean (μ) ± σ calendar position and ^{14}C age ± σ of each of the modeled Therasia and Thera olive (TO) sample dates in their ordered Sequences from Model A_20TOr5 (Figure 3) placed against the IntCal20 calibration curve with curve resolution at 5 years. Data from OxCal 4.4.4 and IntCal20 with curve resolution set at 5 years.*

notable that all models offer relatively similar results (including those using a uniform probability Phase assumption versus an exponential assumption). Those models using a 20 years resolution calibration curve resolution predictably give the widest ranges; in general, for the samples involved here, the models with curve resolution of 1 year or 5 years appear more appropriate. The models including an exploratory possible additional Arizona Laboratory offset allowance yield the latest date ranges but nonetheless largely indicate consonant findings—however, as discussed above, there appears no good reason to include such an additional offset in this case. The total (earliest and latest) 68.3% hpd and 95.4% hpd ranges across all the other models (with curve resolution at 1 or 5 years) reported in Table 2 for the Boundary representing the date of the Thera eruption cover 1613–1585 BC and 1617–1565 BC respectively.

The key issue is where the ordered Sequence data, as a group with each of the outer/bark dates associated within a few calendar years, can best fit against the atmospheric radiocarbon record. Figure 4 shows the mean (μ) ± σ calendar position and ^{14}C age ± σ of each of the modeled Therasia and Thera

https://doi.org/10.1017/RDC.2024.44 Published online by Cambridge University Press

Table 3. *Modeled calendar age ranges for the outermost edge of olive shoot 88-3, the end of growth of the Thera olive branch (Friedrich et al. 2006, 2014), the end Boundary for the stages 2/3 Phase, and the end Boundary representing the dating estimate for the Thera eruption (see Figure 9) from the two models incorporating the Therasia olive sample Sequences, the Thera olive (TO) Sequence, the set of radiocarbon dates on short-lived material from secure stages 2/3 contexts at Akrotiri on Thera, and a Sequence with an assumed very short or short time interval only between the end of stages 2/3 and the timing of the Thera eruption*

Model A_TOr1+2/3	OxCal Am/Ao	hpd	88-3 last, Date BC	TO end Boundary Date BC	End Stages 2/3 Boundary Date BC	Boundary "Eruption", Date BC
LnN(ln(0.75), ln(3))	161/157	68.3%	1615–1605	1616–1606	1615–1603	1613–1602
		95.4%	1619–1594	1621–1598	1620–1586	1618–1584
LnN(ln(3), ln(2))	159/155	68.3%	1614–1605	1616–1606	1617–1605	1612–1602
		95.4%	1618–1595	1621–1598	1621–1593	1616–1589

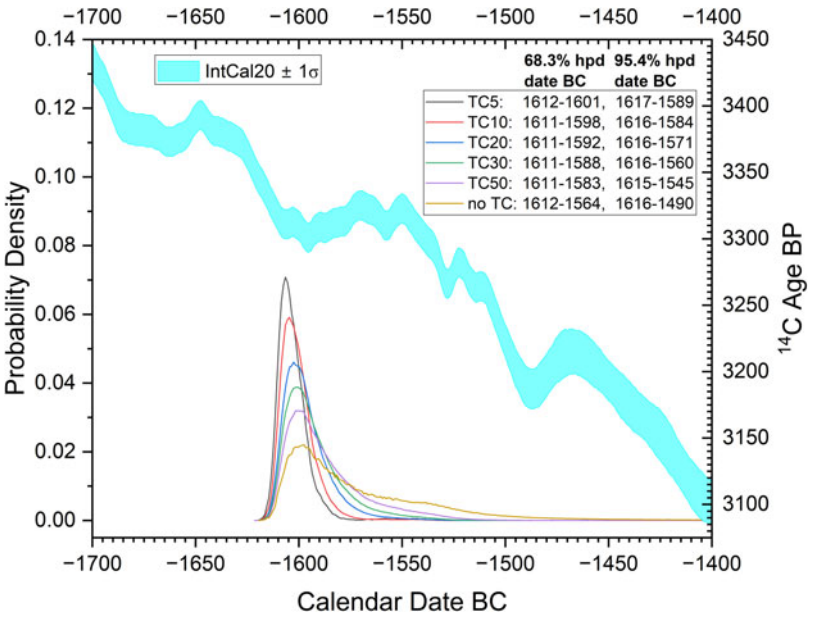

Figure 5. *The modeled probability densities for the Thera eruption Boundary from Model A_r1 with variously a uniform time constant applied to the parameter Tau of 0–5, 0–10, 0–20, 0–30, 0–50 years or no time constant value applied (so Model A_5r1 to Model A_50r1 and Model A_noTCr1). The distributions are shown in relation to IntCal20. The 68.3% hpd and 95.4% hpd ranges for each distribution are listed. Data from OxCal 4.4.4 and IntCal20 with curve resolution set at 1 year.*

olive (TO) sample dates from Model A_20TOr5 (Figure 3) placed against the IntCal20 calibration curve with curve resolution at 5 years. The later 17th century BC alone offers a successful good placement for all the data and is compatible with a plausible total calendar span for each sample Sequence and with the assumption that all the outer/bark dates fall within a relatively similar period (here the constraint is a uniform probability range of 0–20 years). In contrast, although the mid-16th century BC can offer a fit

https://doi.org/10.1017/RDC.2024.44 Published online by Cambridge University Press

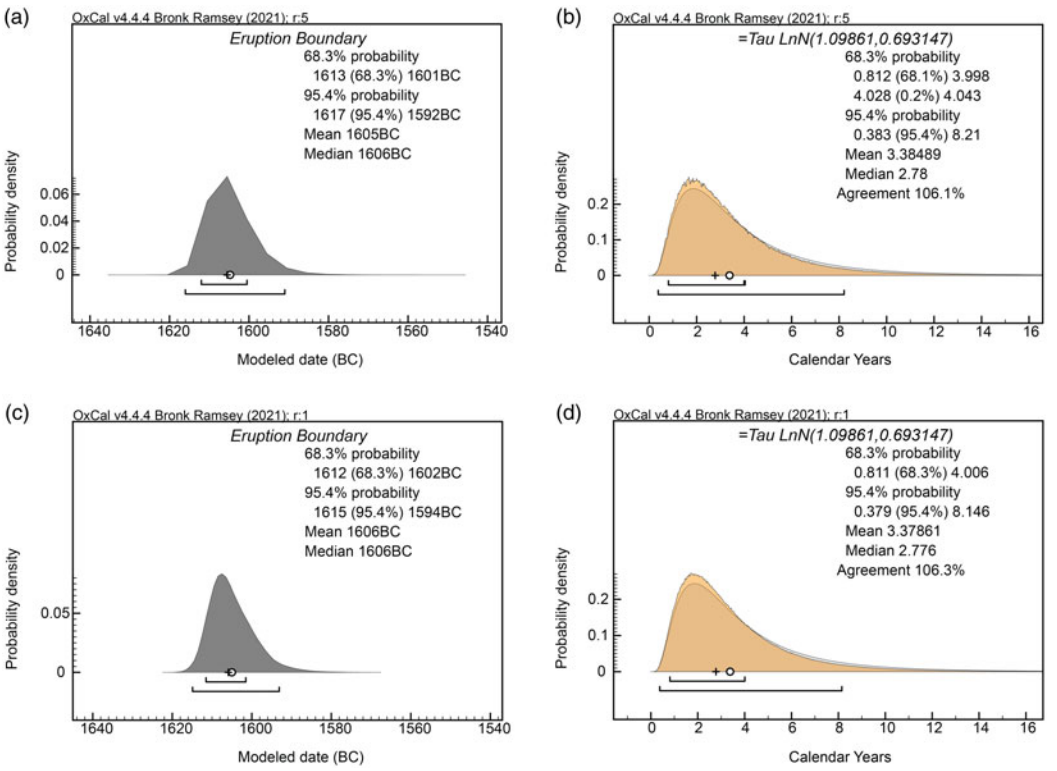

Figure 6. *The modeled probability densities for the Thera eruption Boundary from Model A re-run with an LnN prior of the form LnN(ln(3),ln(2))); applied to the time constant (Tau) for the exponential distribution.* ***a.*** *and* ***b.*** *with calibration curve resolution set at 5 years (Model A_20TOr5_LnN), showing the Eruption Boundary dating probabilities, and the fit of the parameter Tau, the time constant for the exponential distribution, versus the LnN prior.* ***c.*** *and* ***d.*** *as* ***a.*** *and* ***b.****, but with calibration curve resolution set at 1 year (Model A_20TOr1_LnN). Data from OxCal 4.4.4 and IntCal20.*

for the more recent ^{14}C ages, the older values, e.g. those >3340 ^{14}C years BP, progressively offer less successful fits. Unless the sample Sequences are allowed to become much longer than seems plausible (see above), this favors the placement region shown in Figure 4.

Discussion

Calibration Curve Plateau and Date of the Therasia Olive Samples

Dating samples and Sequences with limited constituent members and overall length is challenging where they correspond with a plateau in the radiocarbon calibration curve (Figure 1). The Therasia olive samples offer such a case. Pearson et al. (2023) when presenting these data began by observing this issue and what they referred to as the "plateau effect". Nonetheless, their analysis of the available Sequences ended offering calendar dating probability for the outer growth segments of these samples that spread out "encompassing the late 17th and entire 16th century BC". Within these large ranges they argued that their findings pointed towards a mid-16th century BC date for the final growth of these samples and thus the event that killed them: the Thera volcanic eruption.

However, application of appropriate modeling (e.g. use of Boundaries), use of priors for the plausible time constraints for the overall length of the Sequences represented by each of the Therasia olive samples (from the same olive shrub killed by the Thera eruption), and associating all the outer/bark dates

https://doi.org/10.1017/RDC.2024.44 Published online by Cambridge University Press

as representing approximately the same calendar period within a few years, combine to suggest that calendar probability for the date of the final growth of these samples in fact did not spread right across most of the 16th century BC. Instead, the probability concentrates in the period around and just before 1600 BC. This is a conspicuous difference, basically about half a century, and highlights the need to be very aware of "plateau spread" where applicable, and to try to have a dating and modeling strategy that can attempt to use appropriate informative priors to control against unjustified probability spread across a plateau resulting in potentially incorrect (too old or too recent) calendar age interpretations.

The use of a constraint on the time constant for the Phase of outermost/bark dates is the key issue. The context and nature of the Therasia samples, all from parts of the same olive shrub killed by the Thera eruption, suggests that these final outermost/bark elements should all lie within a very few years of each other. Thus, a time constant with uniform probability of 0–20 years is very conservative, but does act to prevent probability spread. To investigate, Model A with curve resolution set at 1 year was run with time constants applied to the parameter Tau of 0–5, 0–10, 0–20, 0–30, 0–50 years and a final version with no time constraint and the resultant Thera eruption Boundary probability distributions are shown in Figure 5. While the mode of each distribution is similar, as the prior range value is increased (and especially beyond any realistic value, so >20 years to no constraint) the probability spreads (more and more) across the 16th century BC plateau in the radiocarbon calibration curve. But this is entirely unrealistic. The outermost/bark samples should all be within just a few (perhaps even 0–2) calendar years; hence the time constants with 0–5, 0–10 and at most 0–20 years offer the realistic results. These point to 68.3% hpd ranges (overall) from 1612–1592 BC and 95.4% hpd ranges from 1617–1571 BC. As explained in Methods (above), perhaps a more appropriate alternative to the fixed limits of the uniform prior is instead to use a suitable LnN distribution to capture the assumption that we expect all the outermost Therasia olive shrub samples to date within a very similar period of just a couple of years, but without a hard upper limit if in fact the data themselves indicate a longer duration than expected. The eruption date ranges determined using this alternative time constraint from Model A with curve resolutions of 5 years and 1 year are shown in Figure 6. In each case the data conform well with the prior, and the modeled calendar probabilities are very similar to the ranges identified in the other models reported in Figures 2-4 (and Figures S1-S4 in the Supplementary Materials) and Table 2.

Post-Thera-Eruption Terminus ante Quem (TAQ) Information

A number of sites offer radiocarbon dating evidence for a TAQ for the Thera eruption. This evidence either comprises (i) dating of the earliest attested contexts where there are Thera eruption products (pumice) present (likely from craft use): Tell el-'Ajjul in the southern Levant (Fischer 2009) and Tell el-Dab'a in the Nile Delta (Kutschera et al. 2012), or (ii) a date that offers a TAQ for a Thera-associated tsunami (at Malia in Crete) (Lespez et al. 2021), or (iii) the dating of archaeological contexts representing material culture phases that are known stratigraphically to be subsequent to the Thera eruption which is placed in the late Late Cycladic (LC) I or late Late Minoan (LM) IA or late Late Helladic (LH) I cultural periods (Warren and Hankey 1989; Driessen and Macdonald 1997; Manning 1999, 2022; Warburton 2009): thus subsequent LHIIA or LHII contexts at Iklaina (Cosmopoulos et al. 2019), Kakovatos (Eder and Hadzi-Spiliopoulou 2021) (mainland Greece) and Kolonna on Aegina (Wild et al. 2010) or subsequent LMIB contexts at Chania and Myrtos-Pyrgos on Crete (see Manning 2022, 2009—the latter before the LMIB Final dates from Mochlos on Crete).

The extent to which this evidence is a TAQ varies. The short-lived samples from late/end of LMIB destructions on Crete are inherently some time after the Thera eruption. The whole of the LMIB cultural period—potentially a reasonably substantial period of time (Brogan and Hallager 2011)—occurs between the eruption and the end of this subsequent cultural period. The LHIIA or LHII data indicate dating evidence for parts of the LHIIA and LHII periods and again do not indicate the start of the LHIIA period. Thus there is a length of time in the "ante" in the TAQ. The scale of the "ante" in the TAQ from Malia related to a sequence with Thera tsunami deposits is not known. Thera (Minoan eruption) pumice

https://doi.org/10.1017/RDC.2024.44 Published online by Cambridge University Press

appears in both sub-phases of Stratum H5 at Tell el-'Ajjul, thus the eruption likely happened during Stratum H6 and the Boundary (in the site radiocarbon Sequence) representing the transition between Stratum H6 and H5 offers a TAQ for the date of the Thera eruption (with an unknown length of time incorporated into this "ante"). For these short-lived samples and resultant AMS ^{14}C dates from the southern Levant we may assume that an approximate southern Levant growing season offset applies of about 12±5 ^{14}C years (Manning et al. 2020b, 2020c). Minoan pumice was found at Area H in Strata C3 and C2 at Tell el-Dab'a in the Nile Delta region of Eygpt. Thus, the Boundary for the start of Stratum C in the site radiocarbon dating model (Kutschera et al. 2012) offers a TAQ or date for the Thera eruption—again the approximate AMS Egyptian growing season offset of 12±5 ^{14}C years should apply (Manning et al. 2020b, 2020c).

A Phase comprising each of these TAQs derived from radiocarbon dating models for each site (whether as published, e.g. Kutschera et al. 2012—as modified in Höflmayer and Manning 2022; Wild et al. 2010; Manning 2022, or as constructed from published data) is shown in Figure 7 with a start Boundary for this Phase offering an overall range for a TAQ or date for the Thera eruption: 1616–1552 BC (68.3% hpd) and 1665–1538 BC (95.4% hpd). Figure 7 also compares the TAQ ranges with the dates of the V3 (1611 BC) and V5 (1561 BC) volcanic eruptions (Pearson et al. 2022; and see below) and versus the overall (highest/lowest) 68.3% and 95.4% hpd ranges for the Boundary representing the Thera eruption from the models in Table 2 without any Arizona offset correction and for calibration curve resolutions of 1 or 5 years. A reasonably good fit is evident. Those cases where the length of the "ante" in the TAQ should be rather longer (like the late/end LMIB datasets) offer slightly later age ranges. The data and OxCal model used to construct Figure 7 are provided in the Supplementary Material.

Radiocarbon Dating of Sequences from Olive Wood Samples from Therasia and Thera and the Date of the Thera Eruption

The polar ice-core record of larger or climatically effective volcanic eruptions indicates several events that have the potential to represent the Minoan eruption of the Thera volcano (Pearson et al. 2022). In view of the date ranges identified by the models reported in Table 2, the signals reported for 1611 BC (V3), 1586 BC (V4) and 1561 BC (V5) represent the possible Northern Hemisphere (NH) candidates (the eruption V7 dated 1538 BC is clearly well outside all the 95.4% date ranges in Table 2 and thus is not considered as plausible). However, the 1586 BC (V4) eruption is argued to represent a high latitude NH event and thus is unlikely to be Thera. This leaves the eruptions dated 1611 BC (V3) and 1561 BC (V5). As a very large mid-latitude volcanic event, even if its total SO_2 production is not particularly large, it seems likely that Thera should be present in the known ice-core records. Hence it should be one of these two remaining events—although it nonetheless remains a possibility that, for various reasons, Thera is not presently recognized in these ice-core records.

Looking at the model runs using calibration curve resolutions of 1 or 5 years and excluding those adding an additional exploratory Arizona Laboratory offset (discussed above and argued not to be appropriate in this case), the extremes of the reported 68.3% hpd and 95.4% hpd ranges (1613–1585 BC and 1617–1565 BC respectively) only include the 1611 BC eruption signal. However, since the 1561 BC volcanic eruption occurs only a very few years after the latest 95.4% range limits, it clearly remains a possibility. Nonetheless, the most likely 68.3% ranges strongly and only indicate compatibility with the 1611 BC eruption signal (assuming the 1586 BC volcanic eruption is ruled out as high northern latitude and hence is not Thera). If the relatively coeval date ranges for the geochemical signatures from peaks of bromine and molybdenum that likely indicate the Thera eruption in a Sofular Cave speleothem (Badertscher et al. 2014) are included, then these too add to the likelihood for the 1611 BC eruption (or a close-by date within/around the 68.3% hpd ranges in Table 2) (Manning 2022). Figure 8 shows the versions of Model A with the LnN time constraint in Figure 6 re-run with the combined dates for the

https://doi.org/10.1017/RDC.2024.44 Published online by Cambridge University Press

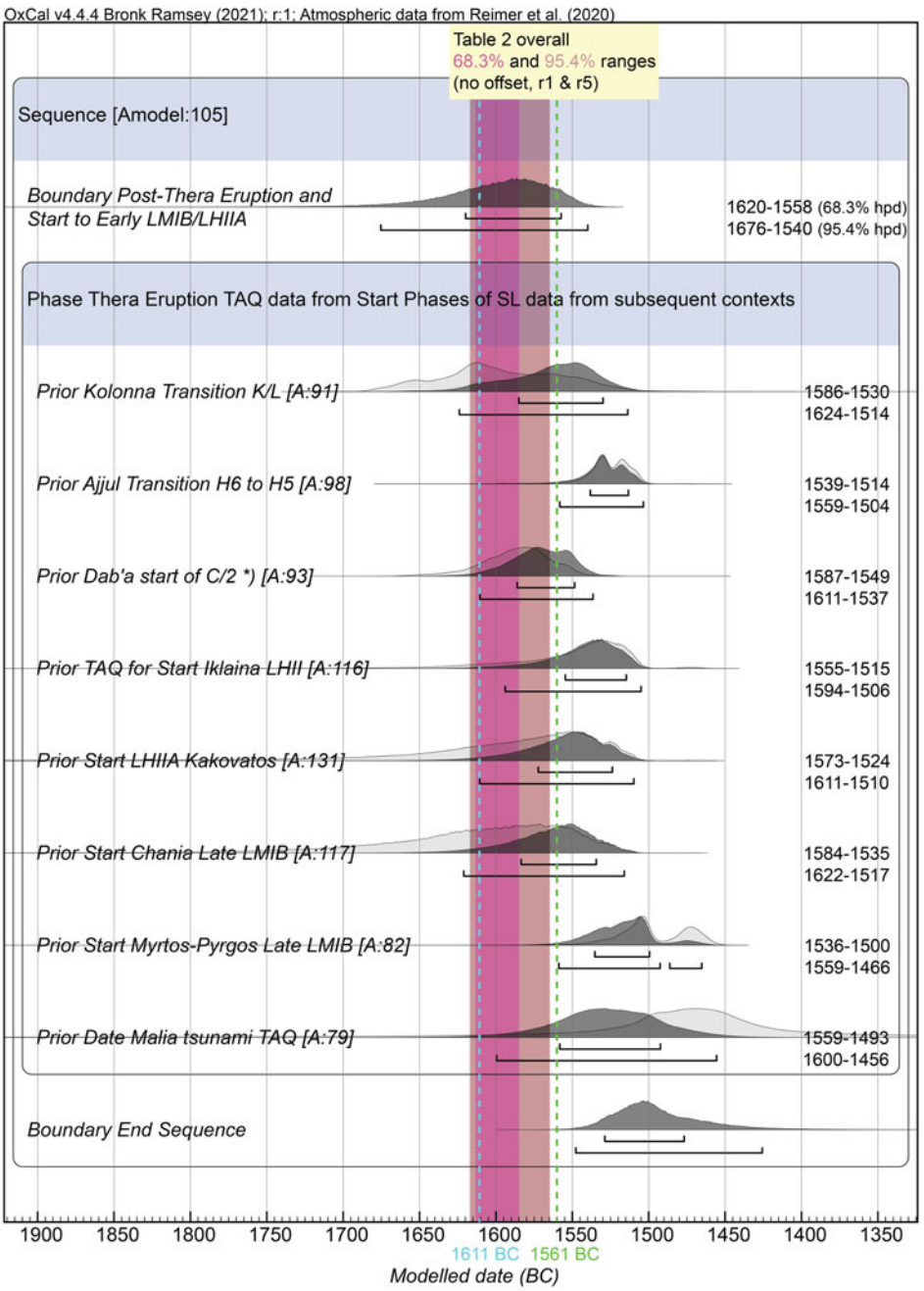

Figure 7. *A Phase showing the Boundaries or a Date query from Sequences of data from various sites and their dating models (see Supplementary Material) that each set a* terminus ante quem *(TAQ) for the Thera volcanic eruption. Some are close TAQs and some involve more substantial periods of time (see text). A Boundary placed before this Phase therefore offers an estimate for the date of the Thera eruption. The various probability density plots are compared with the 68.3% and 95.4% maximum ranges for the date of the Boundary representing the Thera eruption in Table 2 excluding both those models using the exploratory Arizona Laboratory offset and curve resolution of 20 years. The dates for the two plausible mid-lower latitude northern hemisphere (NH) major volcanic eruptions of 1611 BC (V3) and 1561 BC (V5) (Pearson et al. 2022) are also indicated. Data from OxCal 4.4.4 and IntCal20 with curve resolution set at 1 year.*

https://doi.org/10.1017/RDC.2024.44 Published online by Cambridge University Press

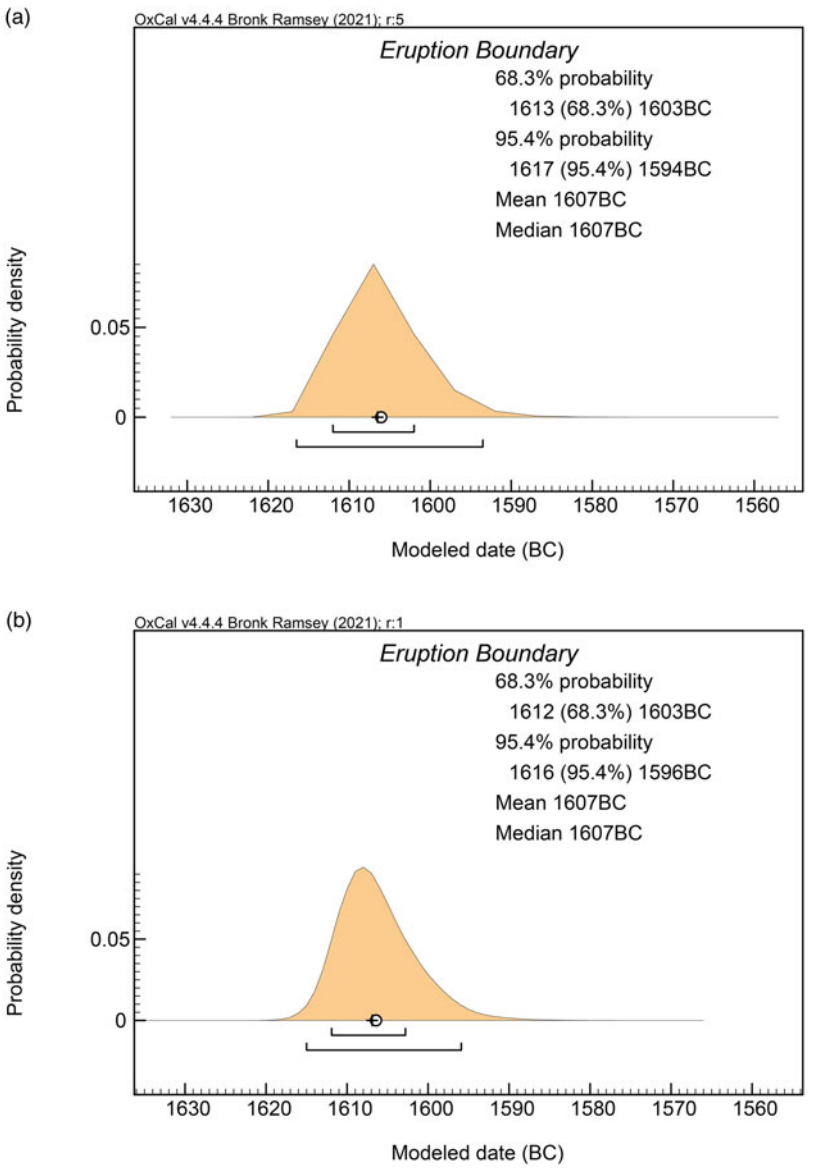

Figure 8. *The two models shown in Figure 6 re-run adding the combined dates for the bromine and molybdenum peaks from the Sofular Cave speleothem (Badertscher et al. 2014) as contributing to the dating probabilities modeled as representing the date of the Thera eruption.* ***a.*** *With curve resolution set at 5 years.* ***b.*** *With curve resolution set at 1 year. Data from OxCal 4.4.4 and IntCal20.*

bromine and molybdenum peaks from the Sofular Cave speleothem added as contributing to the date estimate modeled for the Thera eruption (OxCal code in Supplementary Material).

The Immediate Thera Volcanic Eruption Sequence

As discussed in Manning (2022), there is a specific short-time-period temporal order recorded in the stratigraphy on Thera and at Akrotiri leading to the Thera eruption (Evans and McCoy 2020). In particular, there is a short time period between the abandonment of Akrotiri in stages 2/3 or (ii)/(iii) and

https://doi.org/10.1017/RDC.2024.44 Published online by Cambridge University Press

the final Thera eruption in stage 5 or (v). The stages 2/3 abandonment is dated by the set of short-lived plant samples from foodstuffs left behind stored in jars at the site: 24 samples come from such short-lived (i.e. annual) plants and from definite secure stages 2/3 contexts and one additional sample comes from insect chitin from a seasonally associated pest (*Bruchus rufipes*) (note samples lacking stated contexts and clear stages 2/3 associations were excluded, e.g. K-5353, Hd-6068-5519 and Hd-6059-7967, as was a twig with 10-years growth period: K-4255). Normal traditional agricultural practice and the evidence of food storage pests would suggest that these samples represent the most recent harvest, or perhaps the previous one, and probably not much longer (e.g. 0–2 years window, excepting any possible residual material) and thus offer a date very close to this abandonment episode (Sarpaki 1992; Panagiotakopulu et al. 2013; Manning 2022). This Phase of data may be modeled as exponentially distributed with most data immediately before the abandonment event such that the end Boundary in a Tau_Boundary paired with a Boundary construction gives an estimate for the abandonment episode (e.g. Höflmayer 2012). There is then a very short to short interval in time. Assessments vary, but this is regarded as a relatively short time period covering a timespan somewhere from weeks/months/season(s) up to a period of several years (see Manning 2022). Stage 5 and the eruption follows. The outermost/bark olive wood samples from Therasia should date stage 5 = Thera eruption. So should the estimate for the outermost growth of the Thera olive (Friedrich et al. 2006, 2014).

We can therefore combine (a) the Akrotiri stages 2/3 data with (b) models for the Therasia and Thera olive wood samples with the key chronological constraint that (a) is earlier than (b) but also that (a) is likely within a very short to short time period of (b). This paired temporal prior constraint is used instead of any prior constraint on the time constant for the parameter Tau. As in Manning (2022), an appropriate strategy for this prior constraint appears to be a log-normal distribution with most probability for a very short interval (months to several years) but with some decreasing probability for a longer interval with no hard boundary (since this actual period is not known, only estimated), such that the data can overwhelm the prior assumption if this assumption proves to be inappropriate. Two scenarios are used here (very short and short). First a log-normal distribution with a mode around 2–3 months and a 68.3% hpd range from about half a month to 15 months and a 95.4% range from about 4 days to just under 5 years, and second a log-normal distribution with a mode around 2 years and a standard deviation giving a 68.3% range from <1 year to ≤ 5 years and a 95.4% range from around <0.5 year to around 10 years. Both appear appropriate given expert assessments. These constraints are implemented using OxCal code of the form:

```
Interval("Very Short Interval End Stages 2/3 to Stage 5 and Eruption",
LnN(ln(0.75),ln(3)));
```

or

```
Interval("Short Interval End Stages 2/3 to Stage 5 and Eruption",
LnN(ln(3),ln(2)));
```

The Therasia data are employed following Model A, with the growth band counts used as (conservative estimates of) maximum annual age for each sample, along with the Thera olive (TO) Sequence and calibration curve resolution set at 1 year (so Model ATOr1+2/3). The stage 2/3 data and the OxCal model employed are listed in the Supplementary Material. The date estimates for the Boundary representing the Thera eruption from both models are shown in Figure 9 and selected details of dating ranges from both models are listed in Table 3. These models both provide strong cases for a date range (68.3% hpd highest/lowest dates) 1613–1602 BC (1618–1584 BC at 95.4% hpd). This would be compatible with the 1611 BC (V3) volcanic eruption (Pearson et al. 2022)—or another eruption within a decade or so of ca. 1600 BC. The 1561 BC (V5) volcanic eruption starts to be clearly distinguished as later in this combined analysis.

https://doi.org/10.1017/RDC.2024.44 Published online by Cambridge University Press

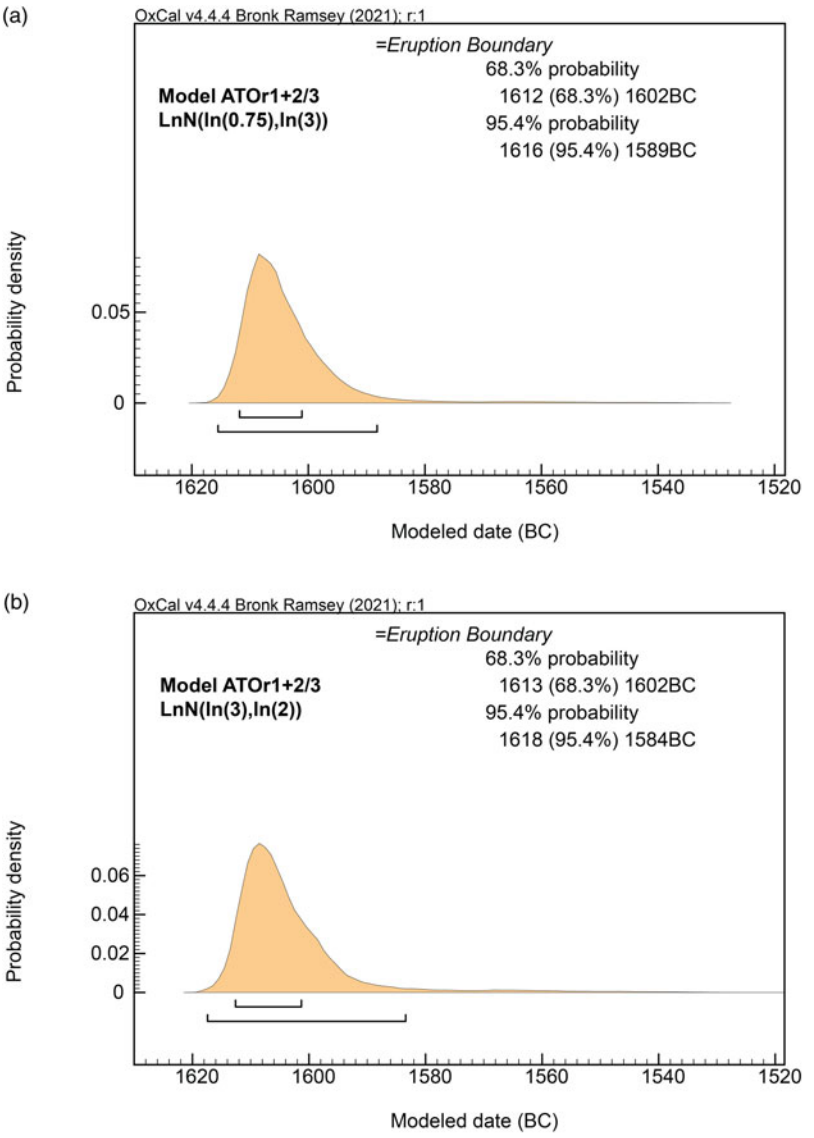

Figure 9. *The modeled Boundary representing the date of the Thera eruption in two versions of a model combining the Therasia sample Sequences, the Thera olive (TO) Sequence, and radiocarbon dates on a set of 25 short-lived samples from secure contexts associated with the end (abandonment) of stages 2/3 at Akrotiri on Thera (for data see Supplementary Material).* ***a.*** *Employs a prior anticipating a very short interval (weeks to months to no more than a very few years) between the abandonment of stages 2/3 at Akrotiri and the main Thera eruption (stage 5) using a LnN(ln(0.75),ln(3)) constraint.* ***b.*** *Employs a prior anticipating a short interval (months to a few to even several years) between the abandonment of stages 2/3 at Akrotiri and the main Thera eruption (stage 5) using a LnN(ln(3),ln(2)) constraint. Data from OxCal 4.4.4 and IntCal20 with curve resolution set at 1 year; for discussion of stratigraphic sequence and modeling, see Manning (2022).*

https://doi.org/10.1017/RDC.2024.44 Published online by Cambridge University Press

The Date of the Thera Eruption?

Definitive (hopefully) dating of the Thera eruption will likely come from recognition of volcanic products specifically (or very likely) from the Minoan eruption of the Thera volcano in a well-dated high-resolution environmental archive: probably an ice-core (and ideally replicated). The recent recognition of Taupo eruption rhyolitic glass shards in the Roosevelt Island Climate Evolution (RICE) ice core (West Antarctica) offers an example (Piva et al. 2023). Until that time radiocarbon can serve to narrow the likely dating window. In recent years it has been suggested that the IntCal20 radiocarbon curve with its much better defined and revised dataset for the period 1700–1480 BC points to a date for the Thera eruption in the mid-16th century BC (e.g. Pearson et al. 2018, 2023). It has been argued in the present paper that this finding is because of the occurrence of the plateau in the radiocarbon calibration curve ca. 1620–1540 BC, coupled with an absence of temporal prior constraints in modeling to prevent inappropriate "plateau spread" affecting the resultant modeled calibrated ranges for radiocarbon dates, and especially Sequences of dates, relevant to dating the Thera eruption.

In contrast, if appropriate prior temporal constraints are applied, the Therasia olive shrub data, whether alone, or combined also with the previous Thera olive data, and both of these combined with the data on short-lived samples from the stages 2/3 abandonment of the Akrotiri archaeological site shortly prior to the Thera eruption, all coherently point to a most likely calendar age range from the very late 17th century BC to early 16th century BC (Tables 2–3, Figures 2–9), probably distinct from the mid-16th century BC (although the eruption about 1561 BC could still be argued to be at, or close to, the latest possible edge of dating probability and especially if any additional small adjustments/offsets come into play). The most likely very late 17th century BC range specifically includes the period of the NH volcanic eruption (V3) dated about 1611 BC from several ice-cores (Pearson et al. 2022).

The Thera eruption has come to form a key time marker in the archaeology and history of the Aegean and East Mediterranean, directly relevant to the remarkable time-capsule buried at the Bronze Age town at Akrotiri on Thera (Palyvou 2005; Doumas et al. 2015) and also many other contexts associated with Thera eruption products or impacts (tephra, pumice, tsunami episodes: e.g. Driessen 2019; Driessen and Macdonald 1997). Material culture and art-style linkages further tie the time horizon of the Thera eruption to archaeological sequences across the wider region (and hence much long-running debate, since the date for the Thera eruption has been uncertain: e.g. Warren and Hankey 1989; Manning 1999, 2022; Sherratt 2000; Warren 2006; Bietak and Höflmayer 2007; Warburton 2009; Höflmayer 2012; Bietak 2013; Manning et al. 2014; Pearson et al. 2018, 2023). A specific date would place these materials and contexts against calendar and thus historical time. Such temporal definition, the when, would then finally allow accurate and robust investigations of cultural, economic, and political relationships and so the questions of why or how. This is the real relevance of the dating question. For just one example: the date for the wall paintings at Akrotiri on Thera (from before the Thera eruption) greatly impacts the likely direction(s) and modality(ies) of associations and influences to be interpreted among the set of Aegeo-Syrian-Egyptian wall paintings known especially from the late Middle Bronze Age to Late Bronze I period from Thera, Alalakh, Qatna, Tel Kabri, and Tell el-Dab'a (Pfälzner 2013; Candelora 2020: 51, 294).

It is important at this point to highlight that no currently available material culture evidence can determine definitively for, or against, a Thera eruption date around e.g. 1611 BC or around e.g. 1561 BC (and today arguments for dates later, in the late 16th century BC, or around 1500 BC, e.g. Bietak 2013, must simply ignore all the substantial body of radiocarbon evidence from multiple loci and laboratories and are hence implausible). The available material culture and textual evidence, examined critically, is either ambiguous, capable of different interpretations, or simply not capable of sustaining the evidential weight necessary to be determinative (e.g. Höflmayer 2012; 2018; Manning et al. 2014; Ritner and Moeller 2014; Manning 2018; Candelora 2020: 23–58). A few key examples suffice:

(i) The famous alabaster lid with the cartouche of the Hyksos ruler Khyan found at Knossos on Crete (Evans 1900/1901: 63–67; Knappett et al. 2023: 149, 169–170; on use of the Hyksos term

https://doi.org/10.1017/RDC.2024.44 Published online by Cambridge University Press

and subsequent titulary by the Hyksos rulers, see Candelora 2017; on Khyan, see Forstner-Müller and Moeller 2018). The find context was for long debated, but is likely Middle Minoan (MM) IIIA (late); however, what is critical is that the dates for Khyan are now likely around a century earlier than previously thought (Höflmayer 2018; generally, see Forstner-Müller and Moeller 2018).

(ii) The low chronology interpretation promulgated for the East Mediterranean by Bietak using his assigned dates for strata at Tell el-Dab'a has been undermined or disproven by radiocarbon dating both at Tell el-Dab'a and other sites, as well as by recent archaeological findings and reassessments (Moeller et al. 2011; Kutschera et al. 2012; Höflmayer 2018; Candelora 2020: 23–58; Höflmayer and Manning 2022; Hermann et al. 2023).

(iii) In contrast to various claims, two Egyptian stone vessels found in the Mycenae Shaft Graves (Warren 2006) cannot be securely placed as New Kingdom (and hence requiring a date for late LHI after some point variously dated ca. 1565–1540 BC, the likely range of dates for the start of the New Kingdom: see Manning 2022), versus potentially Second Intermediate Period (SIP), from the available typological comparanda. Further, critical examination of the basis to key comparanda reveal these to be inadequate to suspect (see Höflmayer 2018: 161).

(iv) An Egyptian stone vessel found at Akrotiri is not a very close match with Egyptian examples and Warren (2006) saw it as early New Kingdom *or* late SIP, leaving its chronological position also as non-determinative (indeed, the other material and stylistic linkages evident at Akrotiri, and for LMIA and LHI period, with the Levant and Cyprus and the world of the SIP could all serve to make SIP dates plausible for this item and those in (iii): e.g. Manning 1999; Merrillees 2009; Höflmayer 2012; Pfälzner 2013; Manning et al. 2014; Candelora 2020: 23–58).

Hence the relevance currently of the radiocarbon dating evidence to resolve ambiguity in Aegean absolute chronology around the period of the Thera volcanic eruption.

As argued and discussed in more detail in Manning (2022), a date of either 1611 BC or 1561 BC for the Thera eruption, late in, or at the close of, the LCI or LMIA or LHI periods, represents substantial change in the conventional historical assumptions and structure. In particular, a date of 1611 BC, or one around 1600 BC (see Figures 2–9, Tables 2–3), shifts the LMIA period (and its contemporaries, like mainland LHI and the Shaft Grave phenomenon) well into the SIP, since the LMIA period ends around the time of the Thera eruption or relatively soon after. Further, since the SIP ends and the New Kingdom of Egypt likely begins sometime between ca. 1565–1540 BC (e.g. Aston 2012; Gautschy 2014; Ritner and Moeller 2014; Manning et al. 2020c), not only the entire LMIA period, but also the earlier portion of the subsequent LMIB period (several decades to even as much as half a century) likely also falls within the timeframe of the late SIP. These temporal associations are very different from the previous, orthodox, Mediterranean history. Here Cretan and Aegean prehistory was constructed on the basis that the early Late Bronze Age (and LMIA) was wholly or largely contemporary with, and parallel/associated with and primarily influenced by, the earlier New Kingdom of Egypt (Evans 1921–1935; Furumark 1950; Hankey and Warren 1974; Betancourt and Weinstein 1976; Warren and Hankey 1989). In contrast, a Thera date of 1611 BC or one around 1600 BC, proposed as likely in this paper, places the contemporary and affective cultural, economic and political context of all but the last portion (mid-later LMIB) of the New Palace Period of Crete (collectively the MMIII to LMIB periods), recognized as the acme of Bronze Age Crete, and the period (MMIII to LMIA) when Crete and especially Knossos was a dominant force in the Aegean region (Wiener 1990; Bevan 2010; Knappett and Nikolakopoulou 2014: 30–31), as firmly within and influenced by and associated with the Hyksos-Levantine world of the SIP (Manning 1999, 2018, 2022; Candelora 2020; Höflmayer 2018)—consistent, for example, with the web of elite linkages and influences evident especially in the later Middle Bronze Age to Late Bronze I among the set of known Aegean-Syrian-Levantine wall-paintings (Pfälzner 2013; Candelora 2020: 51, 294). This re-dating invalidates past orthodoxies and necessitates a different cultural, economic, political, as well as interpretative and explanatory, context for historical syntheses of the mid-second millennium BC Aegean-East Mediterranean across numerous topics and media. In this context we may

https://doi.org/10.1017/RDC.2024.44 Published online by Cambridge University Press

observe that, distinct from the original "high" Aegean chronology suggestion of a Thera date ca. 1628 BC—made before revision/improvement of the radiocarbon calibration curve 1700–1500 BC (e.g. Pearson et al. 2020; Reimer et al. 2020; van der Plicht et al. 2020) with this 1628 BC volcanic signal subsequently identified as associated with Aniakchak II (V2 in Pearson et al. 2022)—a Thera eruption date about 1611 BC or around 1600 BC, can be much more readily acceptable within the existing archaeological and historical understandings and syntheses for the East Mediterranean region (Merrillees 2009: esp. 251; Höflmayer 2012) (for an illustration of the shift in radiocarbon dating probability relevant to the present analysis because of the use of IntCal20 data, see Supplementary Material, Figure S5).

The main historical issue is to recognize and re-insert the key role of the Hyksos world of the southern Levant and Nile Delta (e.g. Oren 1997; Forstner-Müller and Moeller 2018; Candelora 2020) and its mega-site of Tell el-Dab'a (ancient Avaris: Bietak 1996), the "gigantic vortex of Mediterranean trade" (Broodbank 2013: 384) during the SIP as the leading/driving cultural and trading influence of the East Mediterranean. This means changing the orthodox position up to now, where the "The Hyksos have gotten lousy press" (Rutter cited in Balter 2006: 508—on changing scholarly assessments of the Hyksos, see Schneider 2018), as the result of the active vilification and writing out of history pursued by the subsequent Egyptian New Kingdom. This is an important difference. The Egyptian conquest of the Hyksos capital of Avaris/Tell el-Dab'a, the extraordinary 2.5 km^2 super-site and engine of the greater region during the SIP (Broodbank 2013: 383–386), at the beginning of the New Kingdom marks an important historical bifurcation for the wider East Mediterranean region: the Hyksos-Levantine SIP world of the late 18th to earlier 16th centuries BC was replaced by an Egyptian empire that eventually reached into the Levant (Weinstein 1981; Höflmayer 2015).

The date of the Thera eruption supported here, paired with recent re-dating of the earlier Hyksos period centered around king Khyan (Forstner-Müller and Moeller 2018; Moeller et al. 2011; Candelora 2020), domiciles the Minoan MMIII-LMIA (and contemporary Aegean and Cypriot) periods as belonging entirely with the former, pre-New Kingdom SIP world, a key transformative era when, as Broodbank (2013: 383–385) characterizes, Avaris, the Hyksos capital and center, "went super-nova . . . the largest city yet seen in the [Mediterranean] basin by a wide margin . . . for over half a millennium . . . [and] . . . electrified the east Mediterranean . . . as the east Mediterranean's economic super-attractor". This is a very different historical (cultural, political, economic) context in which to conceive the development and "high-water mark" of the polities of mid-second millennium BC Crete and their local Aegean influences and connections driving regional change. The sphere and periphery of the Hyksos-SIP world driven from Tell el-Dab'a/Avaris, ranging from southern Greece (Kolonna on Aegina, Mycenae) to the Cyclades (Akrotiri on Thera), Crete, Rhodes (Trianda), and Cyprus, all variously associated and entangled with East Mediterranean/SIP world contacts and influences as evidenced in material culture and expressions, was clearly transformed through the desire for and receipt of all the associated tangibles and intangibles (MMIII and LMIA to a point during early/earlier LMIB on Crete; Middle Helladic III-Late Helladic I in mainland Greece; Middle Cycladic III-Late Cycladic I in the Cycladic Islands; late Middle Cypriot-Late Cypriot IA on Cyprus). Altogether, this late Middle Bronze Age-early Late Bronze Age era associated with the Hyksos-SIP world, and also the beginnings of the Hittite Old Kingdom and a period of dynamic change, power construction, and likely origins of heroic warriors and epic accounts, in Anatolia to northern Syria and the neighboring Aegean (Morris, 1989; Weeden 2022: 537–550), is conspicuous as a new, different, and increasingly inter-connected phase of substantial local to inter-regional social, political, settlement and economic change across this region (e.g. Graziadio 1998; Shelmerdine 2008; Broodbank 2013: 367, 371; Knapp 2013). In contrast, it is the subsequent decline of Crete and the mainland-centered (Mycenaean) makeover of the Aegean starting in the (mid-later) Minoan LMIB period (and LHIIA on the mainland) and onwards (15th–13th centuries BC) that is contemporary and associated with the post-SIP world of the beginnings, consolidation, and history of the Egyptian New Kingdom empire and also the consolidation and expansion of the formalized Hittite Empire in Anatolia (late 16th–13th centuries BC: Weeden 2022: 558–600).

https://doi.org/10.1017/RDC.2024.44 Published online by Cambridge University Press

Among other ramifications, a Thera eruption date in the very late 17th century BC or early 16th century BC (and e.g. 1611 BC), and so an end for the LMIA period around or not long after this time (the eruption occurs late in the overall LMIA period and likewise late in LHI, but there are indications from some sites and data sets of a subsequent relatively brief final portion of LMIA and LHI, after the abandonment of Akrotiri and the shortly following eruption, and before the LMIB or LHIIA periods: Davis and Cherry 1990; Lolos 1990; Manning 1999: 18, 70–75, 331–332), means that the subsequent LMIB period must be very long and around a century or more in length, since this period does not come to a close until during the earlier-mid 15th century BC (Manning 2022, 2009; Brogan and Hallager 2011). In particular: the considerable temporal extent of the LMIB period—a time period during which regional centrality begins to shift within the Aegean from Crete (Knossos) to various centers in mainland Greece (Knappett and Nikolakopoulou 2014: 31)—renders it problematic to see anything more than a very indirect relationship of the Thera eruption with the much later, or very much later, destructions in Crete that mark the close of LMIB period (Driessen and Macdonald 1997; Driessen 2019). The total evisceration of the island of Thera, which had previously formed a major port and focal communications center with widespread connections within Aegean and East Mediterranean networks, was undoubtedly traumatic to the Aegean regional economic, political and cultural systems (as suggested by the modeling of Knappett et al. 2011). This dramatic change and the associated damage caused by Thera eruption impacts (earthquakes, ashfall, tsunamis) in several susceptible areas of the Aegean region around the close of the LMIA period (Driessen 2019; Şahoğlu et al. 2021) may well form the context for changes and realignments that helped lead to important shifts in regional dynamics across the course of the LMIB period, but cannot be attributed as any direct cause for the much later LMIB destructions on Crete.

Dating on Plateaus in the Radiocarbon Calibration Curve

Plateaus on the radiocarbon calibration curve have long been held to limit dating resolution. However, as illustrated in a range of recent work, and this Therasia case study again highlights, various method strategies using informative priors, as relevant or bespoke to the particular samples and context(s) involved, are now available that much better enable chronological resolution via Bayesian Chronological Modeling for contexts that lie at the time of plateaus in the radiocarbon calibration curve (e.g. Manning et al. 2018a; 2018c; 2019; 2020a; Waddington et al. 2019; Meadows et al. 2020; Birch et al. 2021; Rose et al. 2022; Manning and Birch 2022). With increasing radiocarbon measurement accuracy and precision as standard via rigorous sample pretreatment and modern AMS ^{14}C analysis, and a better (ideally annually informed) radiocarbon calibration curve adding resolution (as already in the period 1700–1500 BC discussed in this paper), the application of such methods promises increasingly to allow high-resolution dating on plateaus almost as effectively as on slopes in the radiocarbon calibration curve.

Supplementary material. To view supplementary material for this article, please visit https://doi.org/10.1017/RDC.2024.44

Acknowledgments. I thank Brita Lorentzen for discussion and comments; I thank the reviewers and editors for their suggestions; and I thank Michael Cosmopoulos for hospitality at the Iklaina Archaeological Project.

Competing interests. The author declares none.

References

Aston DA. 2012. Radiocarbon, wine jars and New Kingdom chronology. *Ägypten und Levante* **22–23**:141–158.

Badertscher S, Borsato A, Frisia S, Cheng H, Edwards RL, Tüysüz O, Fleitmann D. 2014. Speleothems as sensitive recorders of volcanic eruptions—the Bronze Age Minoan eruption recorded in a stalagmite from Turkey. *Earth and Planetary Science Letters* **392**:58–66.

Balter M. 2006. New carbon dates support revised history of ancient Mediterranean. *Science* **312**:508–509.

Bayliss A. 2009. Rolling out revolution: using radiocarbon dating in archaeology. *Radiocarbon* **51**:123–147.

Betancourt PP, Weinstein GA. 1976. Carbon-14 and the beginning of the Late Bronze Age in the Aegean. *American Journal of Archaeology* **80**:329–348.
Bevan A. 2010. Political geography and palatial Crete. *Journal of Mediterranean Archaeology* **23**:27–54.
Bietak M. 1996. *Avaris: the capital of the Hyksos*. London: British Museum Press.
Bietak M, Höflmayer F. 2007. Introduction: high and low chronology. In: Bietak M, Czerny E, editors. *The Synchronisation of Civilisations in the Eastern Mediterranean in the Second Millennium BC – III*. Vienna: Austrian Academy of Sciences. p. 13–27.
Bietak M. 2013. Antagonisms in historical and radiocarbon chronology. In: Shortland AJ, Bronk Ramsey C, editors. *Radiocarbon and the chronologies of Ancient Egypt*. Oxford: Oxbow Books. p. 76–109.
Birch J, Manning SW, Sanft S, Conger MA. 2021. Refined radiocarbon chronologies for Northern Iroquoian site sequences: implications for coalescence, conflict, and the reception of European goods. *American Antiquity* **86**:61–89.
Brogan TM, Hallager E, editors. 2011. *LM IB pottery: relative chronology and regional differences*. Athens: Danish Institute at Athens.
Bronk Ramsey C. 2009a. Bayesian analysis of radiocarbon dates. *Radiocarbon* **51**:337–360.
Bronk Ramsey C. 2009b. Dealing with outliers and offsets in radiocarbon dating. *Radiocarbon* **51**:1023–1045.
Bronk Ramsey C, van der Plicht J, Weninger B. 2001. "Wiggle matching" radiocarbon dates. *Radiocarbon* **43**:381–389.
Broodbank C. 2013. The making of the Middle Sea. *A history of the Mediterranean from the beginning to the emergence of the Classical world*. London: Thames & Hudson.
Camarero JJ, Colangelo M, Gracia-Balaga A, Ortega-Martínez MA, Büntgen U. 2021. Demystifying the age of old olive trees. *Dendrochronologia* **65**:125802.
Candelora D. 2017. Defining the Hyksos: a reevaluation of the title hk3 h3swt and its implications for Hyksos identity. *Journal of the American Research Center in Egypt* **53**:203–221.
Candelora DM. 2020. Redefining the Hyksos: immigration and identity negotiation in the Second Intermediate Period [PhD dissertation]. University of California Los Angeles. https://escholarship.org/uc/item/01d9d70t
Cherubini P, Gartner BL, Tognetti R, Bräker OU, Schoch W, Innes JL 2003. Identification, measurement and interpretation of tree-rings in woody species from Mediterranean climates. *Biological Reviews* **78**:119–148.
Cherubini P, Humbel T, Beeckman H, Gärtner H, Mannes D, Pearson C, Schoch W, Tognetti R, Lev-Yadun S. 2013. Olive tree-ring problematic dating: a comparative analysis on Santorini (Greece). *PLoS ONE* **8**:e54730.
Chiraz M-C. 2013. Growth of young olive trees: water requirements in relation to canopy and root development. *American Journal of Plant Sciences* **4**:1316–1344.
Cosmopoulos M, Allen SE, Riebe DJ, Ruscillo D, Liston M, Shelton C. 2019. New accelerator mass spectrometry ^{14}C dates from the Mycenean site of Iklaina. *Journal of Archaeological Science: Reports* **24**:888–899.
Davis JL, Cherry JF. 1990. Spatial and temporal uniformitarianism in Late Cycladic I: perspectives from Kea and Milos on the Prehistory of Akrotiri. In: DA Hardy, CG Doumas, JA Sakellarakis, PM Warren, editors. Thera and the Aegean World III. Vol. 1: Archaeology. Proceedings of the Third International Congress, Santorini, Greece, 3-9 September 1989. London: The Thera Foundation. p. 185–200.
Deslauriers A, Fonti P, Rossi S, Rathgeber CBK, Gričar J. 2017. Ecophysiology and plasticity of wood and phloem formation. In: Amoroso M, Daniels L, Baker P, Camarero J, editors. Dendroecology. Ecological Studies. Vol. 231. Cham: Springer. p. 13–33.
Doumas CG, Palyvou C, Devetzi A, Boulotis C. 2015. Akrotiri, Thera 17th century BC: a cosmopolitan town 3500 years ago. Athens: Society for the Promotion of Studies on Prehistoric Thera.
Driessen J. 2019. The Santorini eruption. An archaeological investigation of its distal impacts on Minoan Crete. *Quaternary International* **499**:195–204.
Driessen J, Macdonald CF. 1997. The troubled island. Minoan Crete before and after the Santorini eruption. Aegaeum 17. Liège and Austin: Université de Liège and University of Texas at Austin.
Drossopoulos JB, Niavis CA. 1988a. Seasonal changes of the metabolites in the leaves, bark and xylem tissues of olive tree (*Olea europaea.* L). I. Nitrogeneous compounds. *Annals of Botany* **62**:313–320.
Drossopoulos JB, Niavis CA. 1988b. Seasonal changes of the metabolites in the leaves, bark and xylem tissues of olive tree (*Olea europaea.* L). I. Carbohydrates. *Annals of Botany* **62**:321–327.
Eder B, Hadzi-Spiliopoulou G. 2021. Strategies in space: the early Mycenean site of Kakovatos in Triphylia. In: Elder B, Zavadil M, editors. (Social) Place and Space in Early Mycenaean Greece. Vienna: Austrian Academy of Science Press. p. 61–84.
Ehrlich Y, Regev L, Boaretto E. 2021. Discovery of annual growth in a modern olive branch based on carbon isotopes and implications for the Bronze Age volcanic eruption of Santorini. *Scientific Reports* **11**:704.
Evans AJ. 1900/1901. The Palace of Knossos. *The Annual of the British School at Athens* **7**:1–120.
Evans AJ. 1921–1935. *The Palace of Minos at Knossos*. Vols. I–IV. London: Macmillan.
Evans KJ, McCoy FW. 2020. Precursory eruptive activity and implied cultural responses to the Late Bronze Age (LBA) eruption of Thera (Santorini, Greece). *Journal of Volcanology and Geothermal Research* **397**:106868.
Fahrni SM, Southon J, Fuller BT, Park J, Friedrich M, Muscheler R, Wacker L, Taylor RE. 2020. Single-year German oak and Californian bristlecone pine ^{14}C data at the beginning of the Hallstatt Plateau from 856 BC to 626 BC. *Radiocarbon* **62**:919–937.
Fischer PM. 2009. The chronology of Tell el-'Ajjul, Gaza: stratigraphy, Thera, pumice and radiocarbon dating. In: Warburton DA, editor. Time's Up! Dating the Minoan eruption of Santorini. Acts of the Minoan Eruption Chronology Workshop, Sandbjerg, November 2007. Aarhus: Danish Institute at Athens. p. 245–257.

https://doi.org/10.1017/RDC.2024.44 Published online by Cambridge University Press

Forstner-Müller I, Moeller N, editors. 2018. The Hyksos ruler Khyan and the Early Second Intermediate Period in Egypt: problems and priorities of current research. Proceedings of the Workshop of the Austrian Archaeological Institute and the Oriental Institute of the University of Chicago, Vienna, July 4–5, 2014. Wien: Österreichischen Akademie der Wissenschaften.

Friedrich WL, Kromer B, Friedrich M, Heinemeier J, Pfeiffer T, Talamo S. 2006. Santorini eruption radiocarbon dated to 1627–1600 B.C. *Science* **312**:548.

Friedrich WL, Kromer B, Friedrich M, Heinemeier J, Pfeiffer T, Talamo S. 2014. The olive branch chronology stands irrespective of tree-ring counting. *Antiquity* **88**:274–277.

Furumark A. 1950. The Settlement at Ialysos and Aegean History c. 1550–1400 B.C. *Opuscula Archaeologica* **6**:150–271.

Gautschy R. 2014. A reassessment of the absolute chronology of the Egyptian New Kingdom and its "brotherly" countries. *Ägypten und Levante* **24**:141–158.

Graziadio G. 1998. Trade circuits and trade-routes in the Shaft Grave period. Studi Micenei ed Egeo-Anatolici 40: 29–76.

Hamilton WD, Haselgrove C, Gosden C. 2015. The impact of Bayesian chronologies on the British Iron Age. *World Archaeology* **47**:642–660.

Hankey V, Warren, P. 1974. The absolute chronology of the Aegean Late Bronze Age. *Bulletin of the Institute of Classical Studies* **21**:142–152.

Heinemeier J, Friedrich WL, Kromer B, Bronk Ramsey C. 2009. The Minoan eruption of Santorini radiocarbon dated by an olive tree buried by the eruption. In: Warburton DA, editor. Time's Up! Dating the Minoan eruption of Santorini. Acts of the Minoan Eruption Chronology Workshop, Sandbjerg, November 2007. Aarhus: Danish Institute at Athens. p. 285–293.

Herrmann VR, Manning SW, Morgan KR, Soldi S, Schloen D. 2023. New evidence for Middle Bronze Age chronology from the Syro-Anatolian frontier. *Antiquity* **97**:654–673.

Höflmayer F. 2012. The date of the Minoan Santorini eruption: quantifying the "offset". *Radiocarbon* **54**:435–448.

Höflmayer F. 2015. Egypt's "Empire" in the southern Levant during the Early 18th Dynasty. In: Eder B, Pruzsinszky R, editors. Policies of exchange. Political systems and modes of interaction in the Aegean and the Near East in the 2nd millennium B.C.E. Vienna: Austrian Academy of Sciences Press. p. 191–206.

Höflmayer F. 2018. An early date for Khayan and its implications for eastern Mediterranean chronologies. In: Forstner-Müller I, Möller N, editors. The Hyksos ruler Khayan and the Early Second Intermediate Period in Egypt: problems and priorities of current research. Proceedings of the Workshop of the Austrian Archaeological Institute and the Oriental Institute of the University of Chicago, Vienna, July 4–5, 2014. Vienna: Austrian Academy of Sciences Press. p. 143–171.

Höflmayer F, Manning SW. 2022. A synchronized early Middle Bronze Age chronology for Egypt, the Levant, and Mesopotamia. *Journal of Near Eastern Studies* **81**:1–24.

Jacobsson P, Hamilton WD, Cook G, Crone A, Dunbar E, Kinch H, Naysmith P, Tripney B, Xu S. 2018. Refining the Hallstatt Plateau: short-term ^{14}C variability and small scale offsets in 50 consecutive single tree-rings from southwest Scotland dendro-dated to 510–460 BC. *Radiocarbon* **60**:219–237.

Knapp AB. 2013. *The archaeology of Cyprus: from earliest prehistory through the Bronze Age*. Cambridge: Cambridge University Press.

Knappett C, Macdonald CF, Mathioudaki I. 2023. Knossos: From First to Second Palace. An Integrated Ceramic, Stratigraphic and Architectural Study. Supplementary Volume 52. London: The British School at Athens.

Knappett C, Nikolakopoulou I. 2014. Inside out? Materiality and connectivity in the Aegean Archipelago. In: Knapp AB, van Dommelen P, editors. *The Cambridge prehistory of the Bronze and Iron Age Mediterranean*. Cambridge: Cambridge University Press. p. 25–39.

Knappett C, Rivers R, Evans T. 2011. The Theran eruption and Minoan palatial collapse: new interpretations gained from modelling the maritime network. *Antiquity* **85**:1008–1023.

Kuniholm PI. 2014. The difficulties of dating olive wood. *Antiquity* **88**:287–288.

Kutschera W, Bietak M, Wild EM, Bronk Ramsey C, Dee MW, Golser R, Kopetzky K, Stadler P, Steier P, Thanheiser U, Weninger F. 2012. The chronology of Tell el-Daba: a crucial meeting point of ^{14}C dating, archaeology, and Egyptology in the 2nd millennium BC. *Radiocarbon* **54**:407–422.

Lespez L, Lescure S, Saulnier-Copard S, Glais A, Berger J-F, Lavigne F, Pearson C, Virmoux C, Celka SM, Pomadère M. 2021. Discovery of a tsunami deposit from the Bronze Age Santorini eruption at Malia (Crete): impact, chronology, extension. *Scientific Reports* **11**:15487.

Liphschitz N, Lev-Yadun S. 1986. Cambial activity of evergreen and seasonal dimorphics around the Mediterranean. *IAWA* **7**:145–153.

Lolos YG. 1990. On the Late Helladic I of Akrotiri, Thera. In: Hardy DA, Renfrew AC, editors. Thera and the Aegean world III. Volume three: chronology. London: The Thera Foundation. p. 51–56.

Luz AL, Pereira H, Lauw A, Leal S. 2014. Monitoring intra-annual cambial activity based on the periodic collection of twigs – a feasibility study. *Dendrochronologia* **32**:162–170.

Manning SW. 1999. *A Test of Time: the volcano of Thera and the chronology and history of the Aegean and east Mediterranean in the mid-second millennium BC*. Oxford: Oxbow Books.

Manning SW. 2009. Beyond the Santorini eruption: some notes on dating the Late Minoan IB period on Crete, and implications for Cretan-Egyptian relations in the 15th century BC (and especially LMII). In: Warburton DA, editor. Time's Up! Dating the Minoan eruption of Santorini. Acts of the Minoan Eruption Chronology Workshop, Sandbjerg, November 2007. Aarhus: Danish Institute at Athens. p. 207–226.

https://doi.org/10.1017/RDC.2024.44 Published online by Cambridge University Press

Manning SW. 2018. Events, episodes and history: chronology and the resolution of historical processes. In: Nevett L, Whitley J, editors. An Age of Experiment: Classical Archaeology Transformed (1976–2014). Cambridge: McDonald Institute for Archaeological Research. p. 119–137.

Manning SW. 2022. Second Intermediate Period date for the Thera (Santorini) eruption and historical implications. *PloS ONE* **17**(9):e0274835.

Manning SW, Birch J. 2022. A centennial ambiguity: the challenge of resolving the date of the Jean-Baptiste Lainé (Mantle), Ontario, site—around AD 1500 or AD 1600?—and the case for wood-charcoal as a *terminus post quem*. *Radiocarbon* **64**: 279–308.

Manning SW, Birch J, Conger MA, Dee MW, Griggs C, Hadden CS. 2019. Contact-era chronology building in Iroquoia: age estimates for Arendarhonon sites and implications for identifying Champlain's Cahiagué. *American Antiquity* **84**:684–707.

Manning SW, Birch J, Conger MA, Dee MW, Griggs C, Hadden CS, Hogg AG, Ramsey CB, Sanft S, Steier P, Wild EM. 2018a. Radiocarbon re-dating of contact era Iroquoian history in northeastern North America. *Science Advances* **4**(12):eaav0280.

Manning SW, Birch J, Conger MA, Sanft S. 2020a. Resolving time among non-stratified short-duration contexts on a radiocarbon plateau: possibilities and challenges from the AD 1480–1630 example and northeastern North America. *Radiocarbon* **62**:1785–1807.

Manning SW, Griggs C, Lorentzen B, Bronk Ramsey C, Chivall D, Jull AJT, Lange TE. 2018b. Fluctuating radiocarbon offsets observed in the southern Levant and implications for archaeological chronology debates. *Proceedings of the National Academy of Sciences of the United States of America* **115**:6141–6146.

Manning SW, Höflmayer F, Moeller N, Dee MW, Bronk Ramsey C, Fleitmann D, Higham T, Kutschera W, Wild EM. 2014. Dating the Thera (Santorini) eruption: archaeological and scientific evidence supporting a high chronology. *Antiquity* **88**:1164–1179.

Manning SW, Kromer B, Cremaschi M, Dee MW, Friedrich R, Griggs C, Hadden CS. 2020b. Mediterranean radiocarbon offsets and calendar dates for prehistory. *Science Advances* **6**:eaaz1096.

Manning SW, Smith AT, Khatchadourian L, Badalyan R, Lindsay I, Greene A, Marshall M 2018c. A new chronological model for the Bronze and Iron Age South Caucasus: radiocarbon results from Project ArAGATS, Armenia. *Antiquity* **92**:1530–1551.

Manning SW, Wacker L, Büntgen U, Bronk Ramsey C, Dee MW, Kromer B, Lorentzen B, Tegel W. 2020c. Radiocarbon offsets and old world chronology as relevant to Mesopotamia, Egypt, Anatolia and Thera (Santorini). *Scientific Reports* **10**:41598.

Meadows J, Martinelli N, Nadeau MJ, Citton EB. 2014. Este, Padova, Italy: dating the Iron Age waterfront. *Radiocarbon* **56**: 655–665.

Meadows J, Rinne C, Immel A, Fuchs K, Krause-Kyora B, Drummer C. 2020. High-precision Bayesian chronological modeling on a calibration plateau: the Niedertiefenbach Gallery grave. *Radiocarbon* **62**:1261–1284.

Merrillees RS. 2009. Chronological conundrums: Cypriot and Levantine imports from Thera. In: Warburton DA, editor. Time's Up! Dating the Minoan eruption of Santorini. Acts of the Minoan Eruption Chronology Workshop, Sandbjerg, November 2007. Aarhus: Danish Institute at Athens. p. 247–251.

Moeller N, Marouard G, Ayers N. 2011. Discussion of late Middle Kingdom and early Second Intermediate Period history and chronology in relation to the Khayan sealings from Tell Edfu. *Ägypten und Levante* **21**:87–121.

Morris SP. 1989. A tale of two cities: the miniature frescoes from Thera and the origins of Greek poetry. *American Journal of Archaeology* **93**:511–535.

Oren E, editor. 1997. *The Hyksos: new historical and archaeological perspectives*. Philadelphia: University Museum, University of Pennsylvania.

Palyvou C. 2005. *Akrotiri Thera: an architecture of affluence 3,500 years old*. Philadelphia: INSTAP Academic Press.

Panagiotakopulu E, Higham T, Sarpaki A, Buckland P, Doumas C. 2013. Ancient pests: the season of the Santorini Minoan volcanic eruption and a date from insect chitin. *Naturwissenschaften* **100**: 683–689.

Pearson C, Sbonias K, Tzachili I, Heaton T. 2023. Olive shrub buried on Therasia supports a mid-16th century BCE date for the Thera eruption. *Scientific Reports* **13**:6994.

Pearson C, Sigl M, Burke A, Davies S, Kurbatov A, Severi M, Cole-Dai J, Innes H, Albert PG, Helmick M. 2022. Geochemical ice-core constraints on the timing and climatic impact of Aniakchak II (1628 BCE) and Thera (Minoan) volcanic eruptions. PNAS Nexus 1:pgac048

Pearson C, Wacker L, Bayliss A, Brown D, Salzer M, Brewer P, Bollhalder S, Boswijk G, Hodgins G. 2020. Annual variation in atmospheric ^{14}C between 1700 BC and 1480 BC. *Radiocarbon* **62**:939–952.

Pearson CL, Brewer PW, Brown D, Heaton TJ, Hodgins GWL, Jull AJT, Lange T, Salzer MW. 2018. Annual radiocarbon record indicates 16th century BCE date for the Thera eruption. *Science Advances* **4**:eaar8241.

Pfälzner P. 2013. The Qatna wall paintings and the formation of Aegeo-Syrian art. In: Aruz J, Graff SB, Rakic Y, editors. Cultures in Contact: From Mesopotamia to the Mediterranean in the Second Millennium B.C. New York: The Metropolitan Museum of Art. p. 200–213.

Piva SB, Barker SJ, Iverson NA, Winton VHL, Bertler NAN, Sigl M, Wilson CJN, Dunbar NW, Kurbatov AV, Carter L, Charlier BLA, Newnham RM. 2023. Volcanic glass from the 1.8ka Taupō eruption (New Zealand) detected in Antarctic ice at ~230 CE. *Scientific Reports* **13**:16720.

Quarta G, Pezzo MI, Marconi S, Tecchiati U, Elia MD, Calcagnile L. 2010. Wiggle-match dating of wooden samples from Iron Age sites in Northern Italy. *Radiocarbon* **52**:915–923.

Raj H, Ehrlich Y, Regev L, Mintz E, Boaretto E. 2023b. Sub-Annual bomb radiocarbon records from trees in northern Israel. *Scientific Reports* **13**:18851.

https://doi.org/10.1017/RDC.2024.44 Published online by Cambridge University Press

Raj H, Regev L, Boaretto E. 2023a. Calibration of multiple tree-ring blocks and its implication on the debate of Minoan eruption of Santorini around 17th–16th century BCE. Radiocarbon 65:681–691.

Reimer PJ, et al. 2020. The IntCal20 Northern Hemisphere radiocarbon age calibration curve (0–55 cal kBP). *Radiocarbon* **62**:725–757.

Ritner RK, Moeller N. 2014. The Ahmose "Tempest Stela," Thera and comparative chronology. *Journal of Near Eastern Studies* **73**:1–19.

Rose HA, Müller-Scheeßel N, Meadows J, Hamann C. 2022. Radiocarbon dating and Hallstatt chronology: a Bayesian chronological model for the burial sequence at Dietfurt an der Altmühl "Tennisplatz", Bavaria, Germany. *Archaeological and Anthropological Sciences* **14**:72 https://doi.org/10.1007/s12520-022-01542-1.

Şahoğlu V, Sterba JH, Katz T, Çayır Ü, Gündoğan Ü, Tyuleneva N, Tuğcu İ, Bichler M, Erkanal H, Goodman-Tchernov BN. 2021. Volcanic ash, victims, and tsunami debris from the Late Bronze Age Thera eruption discovered at Çeşme-Bağlararası (Turkey). *Proceedings of the National Academy of Sciences of the United States of America* **119**:e2114213118.

Sarpaki A. 1992. A palaeoethnobotanical study of the West House, Akrotiri, Thera. The Annual of the British School at Athens 87:219–230.

Sbonias K, Tzachili I, Efstathiou M, Palyvou C, Athanasiou C, Farinetti E, Moullou D. 2020. The Early and Middle Bronze Age settlement at Koimisis, Therasia: periods of habitation and architecture. *The Annual of the British School at Athens* **115**:105–132.

Schneider T. 2018. Hyksos research in Egyptology and Egypt's public imagination: a brief assessment of fifty years of assessments. *Journal of Egyptian History* **11**:73–86.

Shelmerdine CW. 2008. *The Cambridge Companion to the Aegean Bronze Age*. Cambridge: Cambridge University Press.

Sherratt S, editor. 2000. The Wall Paintings of Thera. Proceedings of the First International Symposium, Petros M. Nomikos Conference Centre, Thera, Hellas, 30 August - 4 September 1997. Athens: Petros M. Nomikos and The Thera Foundation.

Steier P, Rom W. 2000. The use of Bayesian statistics for ^{14}C Dates of chronologically ordered samples: a critical analysis. *Radiocarbon* **42**: 183–198.

van de Plassche O, Edwards RJ, van der Borg K, de Jong AFM. 2001. ^{14}C wiggle-match dating in high-resolution sea-level research. *Radiocarbon* **43**:391–402.

van der Plicht J, Bronk Ramsey C, Heaton TJ, Scott EM, Talamo S. 2020. Recent developments in calibration for archaeological and environmental samples. *Radiocarbon* **62**:1095–1117.

Waddington K, Bayliss A, Higham T, Madgwick R, Sharples N. 2019. Histories of deposition: creating chronologies for the Late Bronze Age-Early Iron Age transition in Southern Britain. *Archaeological Journal* **176**:84–133.

Warburton DA, editor. 2009. Time's Up! Dating the Minoan eruption of Santorini. Acts of the Minoan Eruption Chronology Workshop, Sandbjerg, November 2007. Aarhus: Danish Institute at Athens.

Warren P, Hankey V. 1989. *Aegean Bronze Age chronology*. Bristol: Bristol Classical Press.

Warren, PM. 2006. The date of the Thera eruption in relation to Aegean-Egyptian interconnections and the Egyptian historical chronology. In Czerny E, Hein I, Hunger H, Melman D, Schwab A, editors. Timelines. Studies in Honour of Manfred Bietak, Vol. II. Leuven-Paris: Peeters. p. 305–321.

Weeden M. 2022. The Hittite empire. In: Radner K, Moeller N, Potts DT, editors, The Oxford History of the Ancient Near East. Oxford: Oxford University Press. p. 529–622.

Weinstein JM. 1981. The Egyptian Empire in Palestine: a reassessment. *Bulletin of the American Schools of Oriental Research* **241**:1–28.

Wiener MH. 1990. The isles of Crete? The Minoan thalassocracy revisited. In Hardy DA, Doumas CG, Sakellarakis JA, Warren PM, editors. Thera and the Aegean World 3. Volume I: archaeology. London: Thera and the Aegean World. p. 128–161.

Wiener MH. 2012. Problems in the measurement, calibration, analysis, and communication of radiocarbon dates (with special reference to the prehistory of the Aegean world). *Radiocarbon* **54**:423–434.

Wild EM, Gauß W, Forstenpointner G, Lindblom M, Smetana R, Steier P, Thanheiser U, Weninger F. 2010. ^{14}C dating of the Early to Late Bronze Age stratigraphic sequence of Aegina Kolonna, Greece. *Nuclear Instruments and Methods in Physics Research B* **268**:1013–1021.

Cite this article: Manning SW (2024). Problems of Dating Spread on Radiocarbon Calibration Curve Plateaus: The 1620–1540 BC Example and the Dating of the Therasia Olive Shrub Samples and Thera Volcanic Eruption. *Radiocarbon* **66**, 341–370. https://doi.org/10.1017/RDC.2024.44